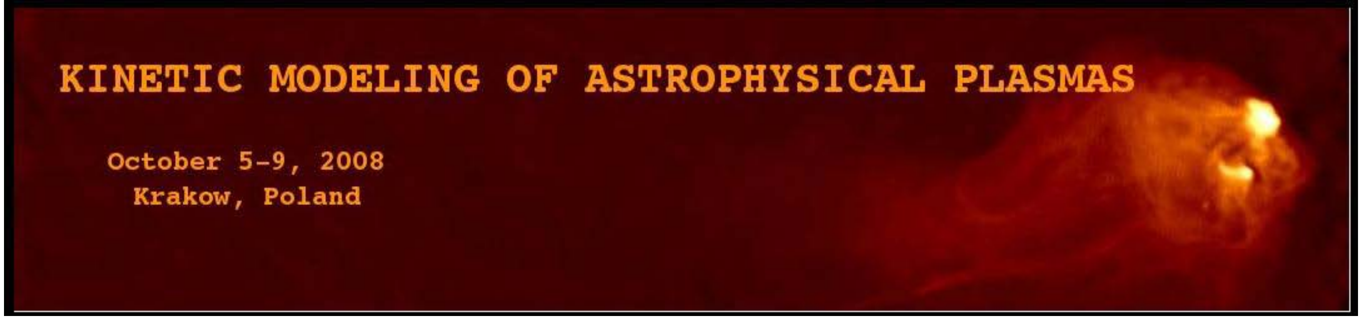

Collisionless Nonrelativistic Shocks – Overview

Manfred Scholer

Max-Planck-Institut für extraterrestrische Physik
Garching, Germany

Tom Gold, 1953: Solar flare plasma injection creates a thin collisionless shock

Norman F. Ness, 1964: Discovery of Earth‘s bow shock from IMP-1 magnetic field data

Important Parameters

Shock normal angle Θ_{Bn}

Trajectories of specularly reflected ions

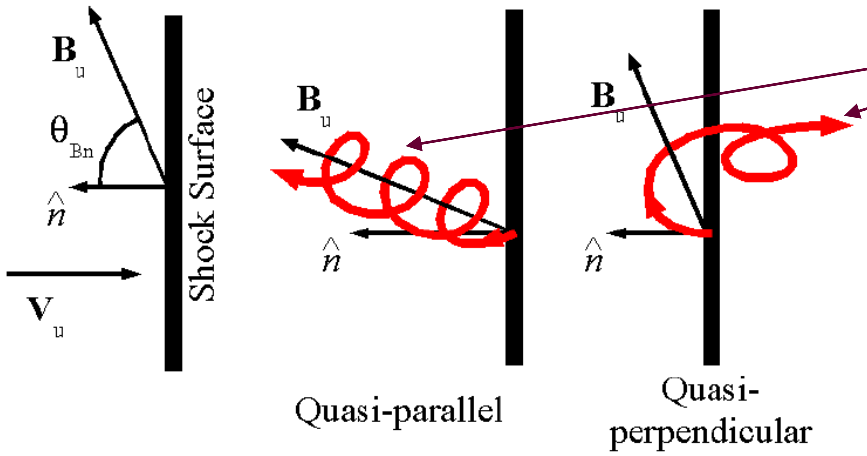

Mach number M_A

Ion/electron beta

Composition, anisotropy

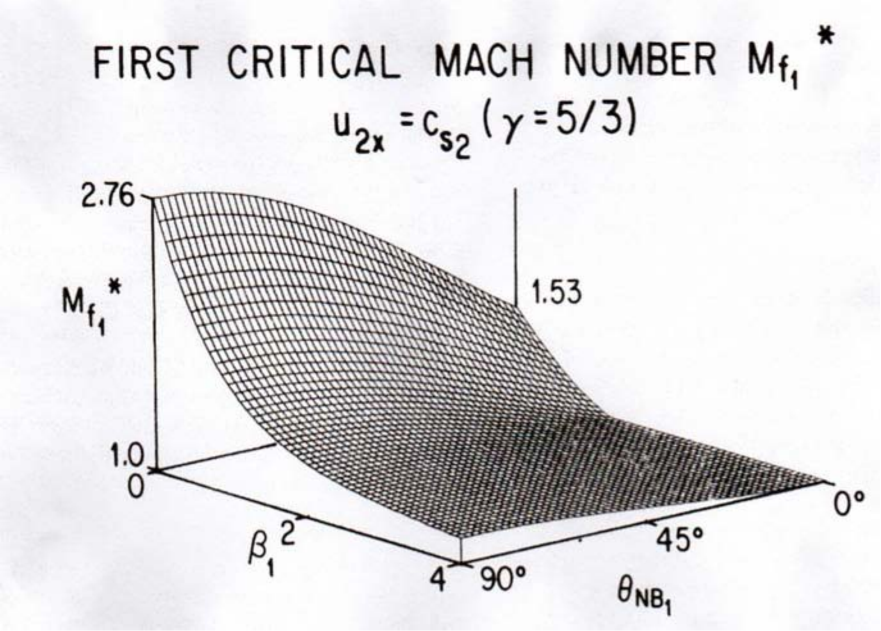

Kennel et al. 1985

Above first critical Mach number resistivity (by whatever mechanism, e.g. ion sound anomalous resistivity) cannot provide all the dissipation required by the Rankine-Hugoniot conditions. Conclusion: additional dissipation needed - particle reflection.

Whistler critical Mach number

$$M_w = \frac{|\cos\Theta_{Bn}|}{2(m_e/m_i)^{1/2}}$$

Upper limit fast Mach number for wich a (linear) whistler can phase stand in the flow

Quasi-Parallel Collisionless Shocks

Parker (1961): Collisionless parallel shock is due to firehose instability when upstream plasma penetrates into downstream plasma

Golden et al. (1973) Group standing ion cyclotron mode excited by interpenetrating beam produces turbulence of parallel shock waves

Early papers did not recognize importance of backstreaming ions

1. Excitation of upsteam waves and downstream convection
2. Upstream vs downstream directed group velocity
3. Mode conversion of waves at shock
4. Interface instability
5. Short Large Amplitude Magnetic Structures (SLAMSs)
6. Injection and diffusive acceleration

Hybrid Simulation of 1-D or 2-D Planar Collisionless Shocks

Inject a thermal distribution from the left hand side of a numerical box
Let these ions reflect at the right hand side
The (collective) interaction of the incident and reflected ions results eventually in a shock which travels to the left

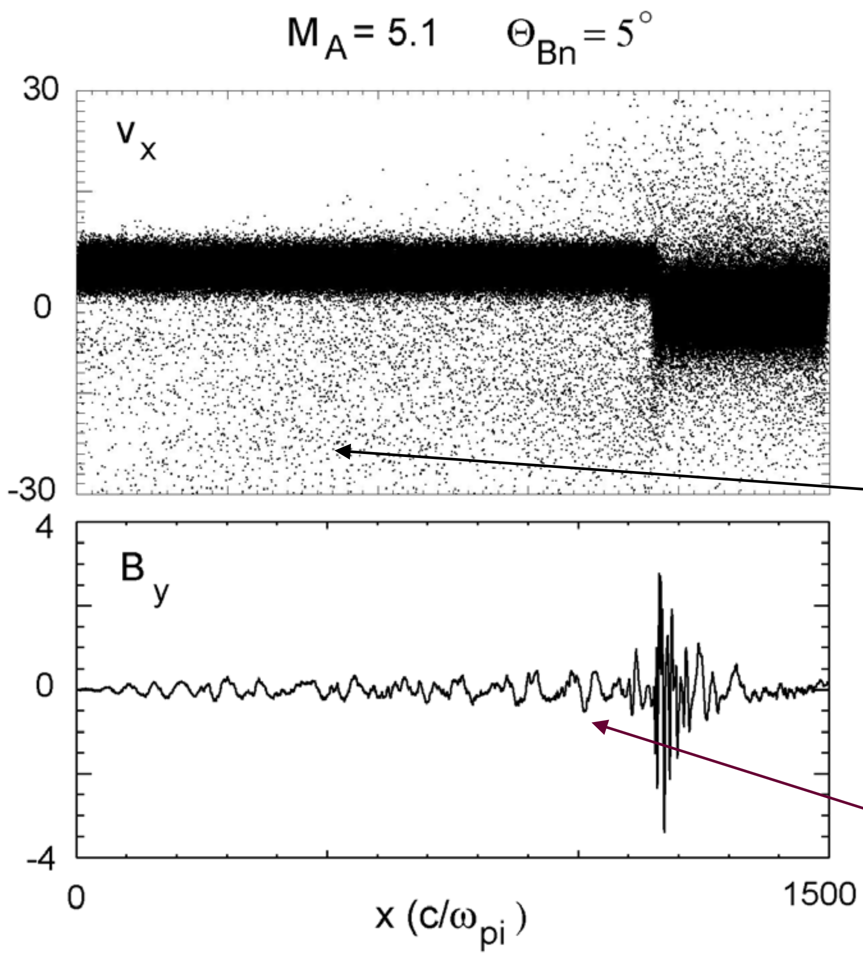

Ion phase space v_x - x
(velocity in units of Mach number)

Diffuse ions

Transverse magnetic field component

Large amplitude waves

$\delta B/B \sim 1$

Electromagnetic Ion/Ion Instabilities

Gary, 1993

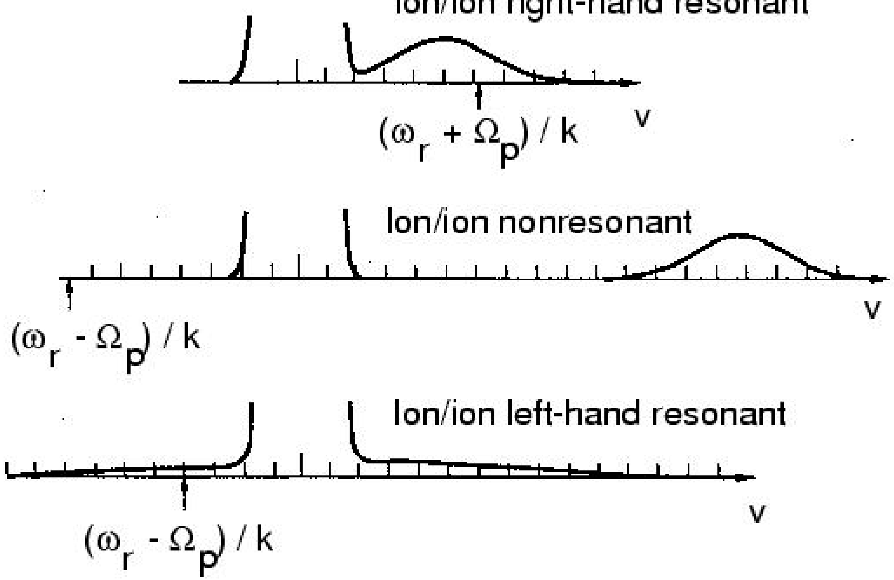

Ion distribution functions and associated cyclotron resonance speed.

Ion/ion right hand resonant
(cold beam)
propagates in direction of beam
resonance with beam ions
right hand polarized
fast magnetosonic mode branch

Ion/ion nonresonant
(large relative velocity, large beam density)
Firehose-like instability
propagates in direction opposite to beam

Ion/ion left hand resonant
(hot beam)
propagates in direction of beam
resonance with hot ions flowing antiparallel to beam
left hand polarized
on Alfven ion cyclotron branch

Upstream Waves: Resonant Ion/Ion Beam Instability

Backstreaming ions excite upstream propagating waves by a resonant ion/ion beam instability

Cyclotron resonance condition for beam ions

$$\omega - k_r v_b = -\Omega_c$$

dispersion relation

$$\omega = k v_A$$

assume beam ions are specularly reflected

$$v_b = 2 v_{sw}$$

(ω in units of Ω_c , k in units of Ω_c / v_A)

$$\omega_r = k_r = 1/(2M_A - 1)$$

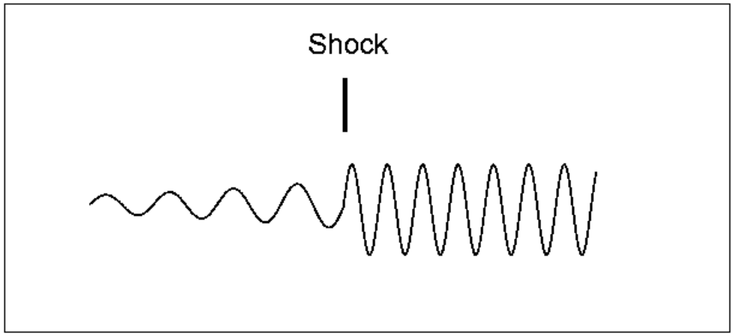

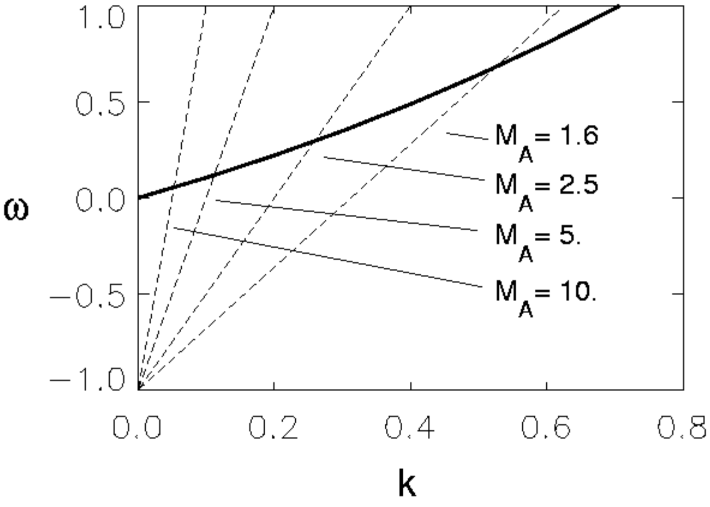

Wavelength (resonance) increase with increasing Mach number

Dopplershift into Shock Frame

(positive ω phase velocity directed upstream)

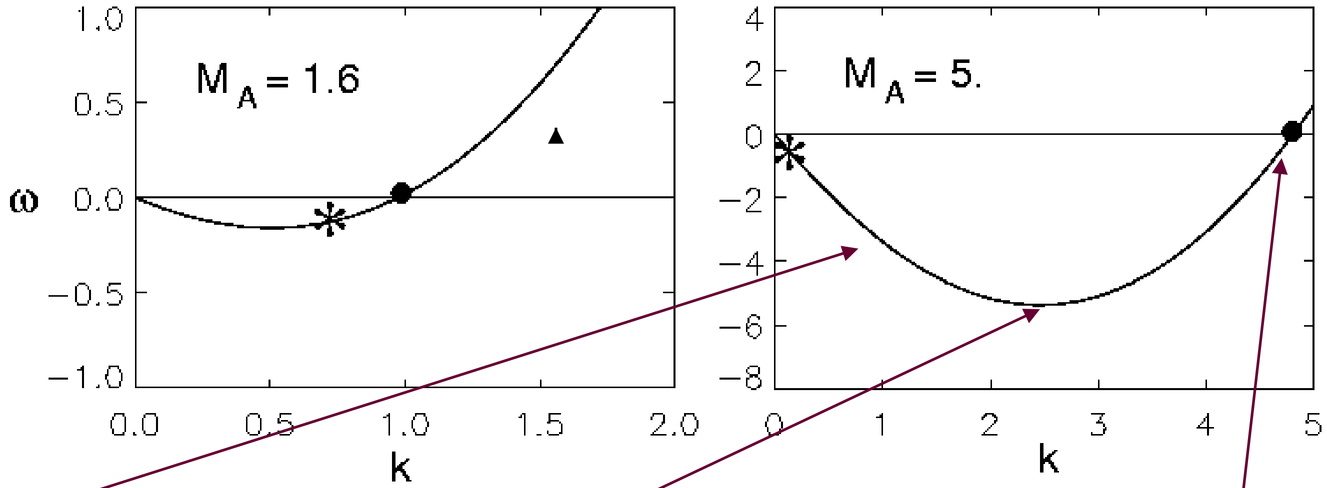

Downstream directed group velocity

Group standing

Phase standing

Dispersion relation of upstream propagating whistler in shock frame.

Dispersion curve is shifted below zero frequency line.

At low Mach number waves (with large k) have upstream directed group velocity; they are phase-standing or have downstream directed phse velocity.

At higher Mach number the group velocity is reduced until it points back toward shock

Upstream wave spectra (2-D (x-t space) Fourier analysis) for simulated shocks of three different Mach numbers

Krauss-Varban and Omidi 1991

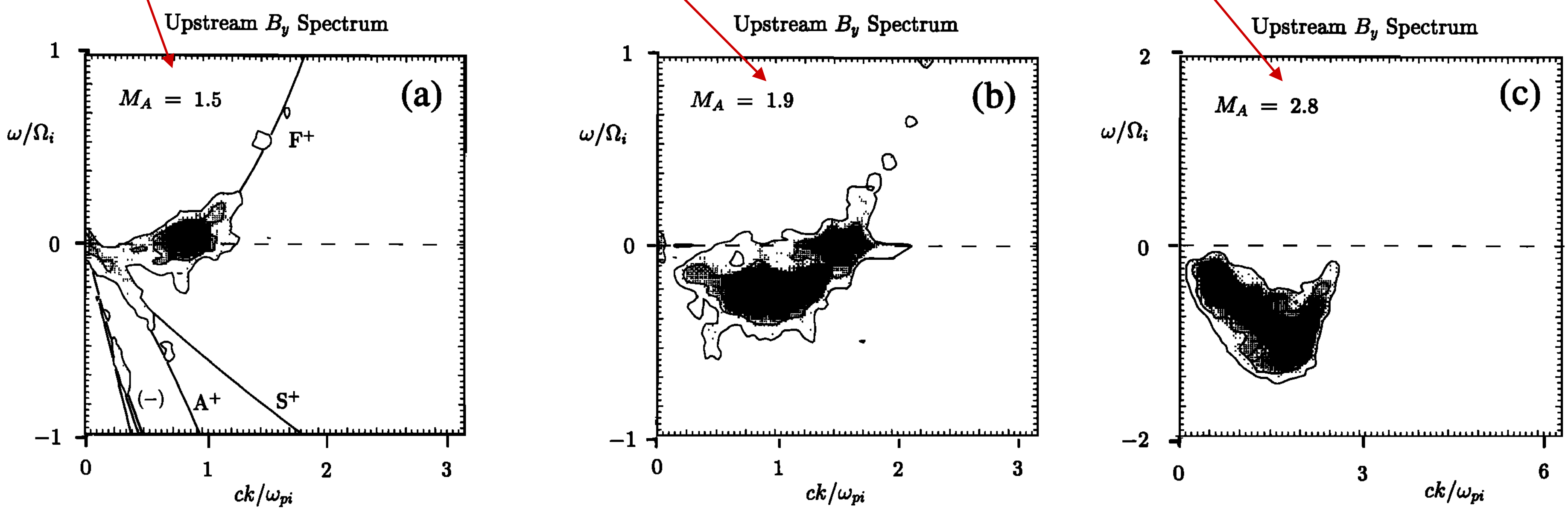

Upstream waves are close to phase-standing. Group velocity directed upstream

Upstream waves are close to group standing.

Group and phase velocity directed towards shock

Shock periodically reforms itself when group velocity directed downstream

Mode Conversion of Upstream Fast Magnetosonic Waves

Krauss-Varban and Omidi 1991

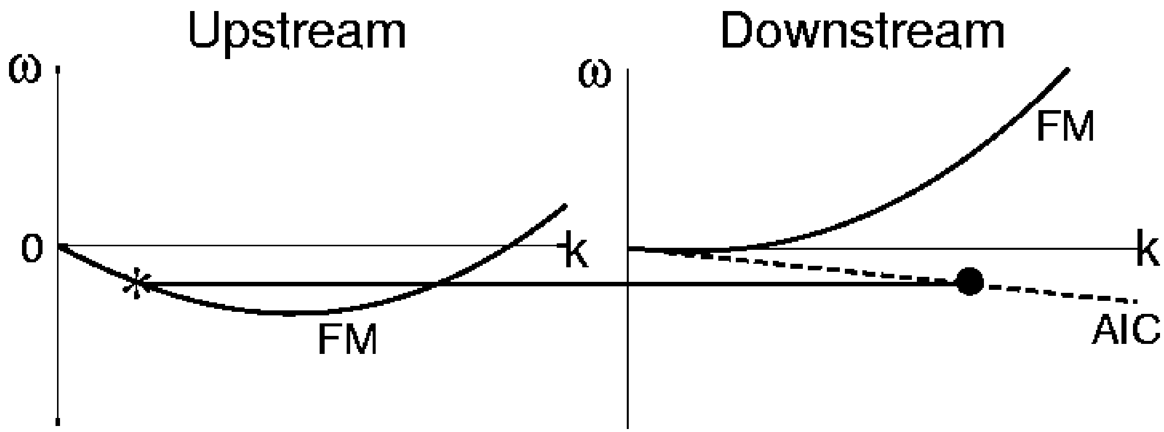

Doppler shifted dispersion relation of upstream propagating fast magnetosonic mode (FM) in upstream region

Doppler shifted dispersion relation of upstream propagating FM and Alfven ion cyclotron mode (AIC) in downstream region

Star * shows position of an upstream wave on the FM branch which is downstream only accessable to the AIC branch (assuming constant wave frequency during shock transmission)

Interface Instability

Winske et al. 1990

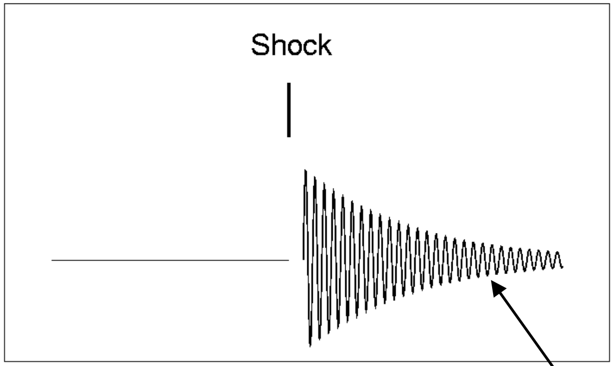

In the region of overlap between cold solar wind and heated downstream plasma waves are produced by a right hand resonant instability (solar wind is background, hot plasma is beam).

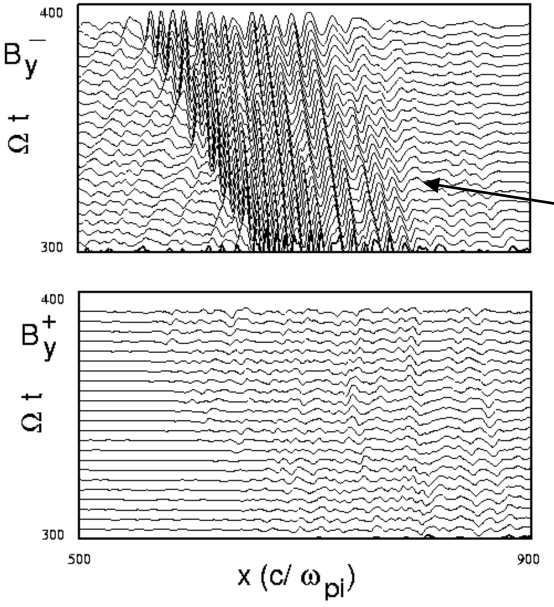

Wave damping

Medium Mach number shock: decomposition in positive and negative helicity

Scholer, Kucharek, Jayanti 1997

Medium Mach Number Shock ($2.5<M_A<7$)

Krauss-Varban and Omidi 1991

Interface waves have small wavelength and are heavily damped

Far downstream only upstream generated F/MS waves survive

F/MS waves are mode converted into AIC waves

Right: wavelet analysis of magnetic field of a M_A=3.5 shock). Two different wavelet components.

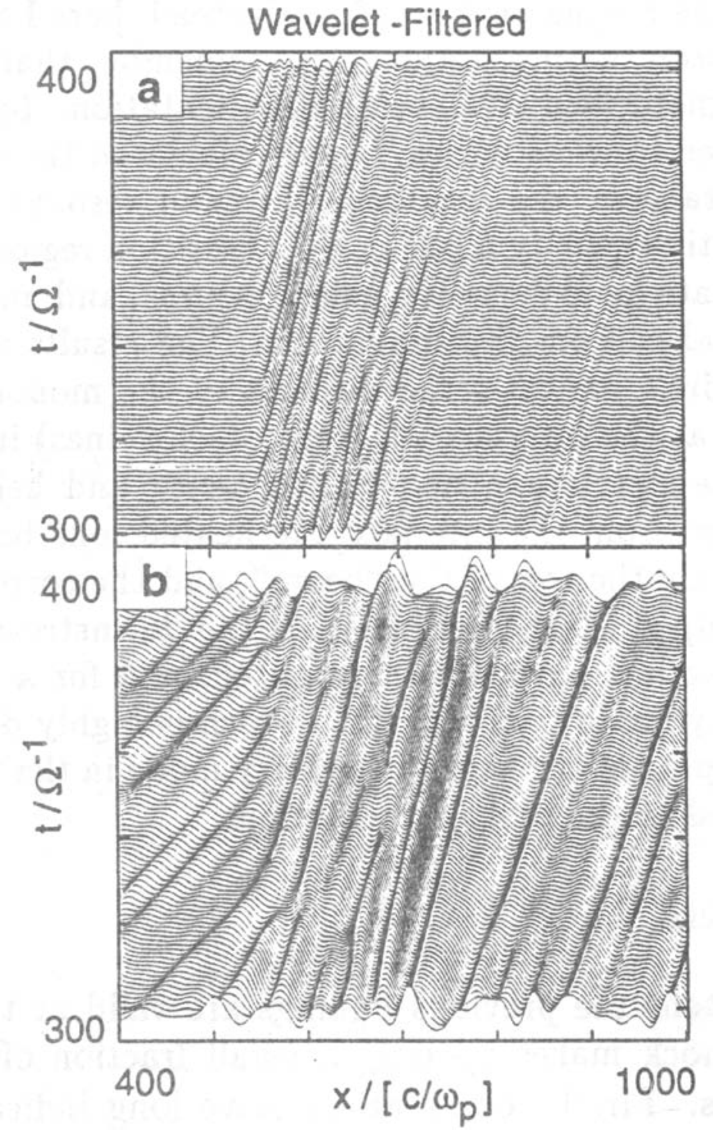

Interface Instability – High Mach Number Shocks

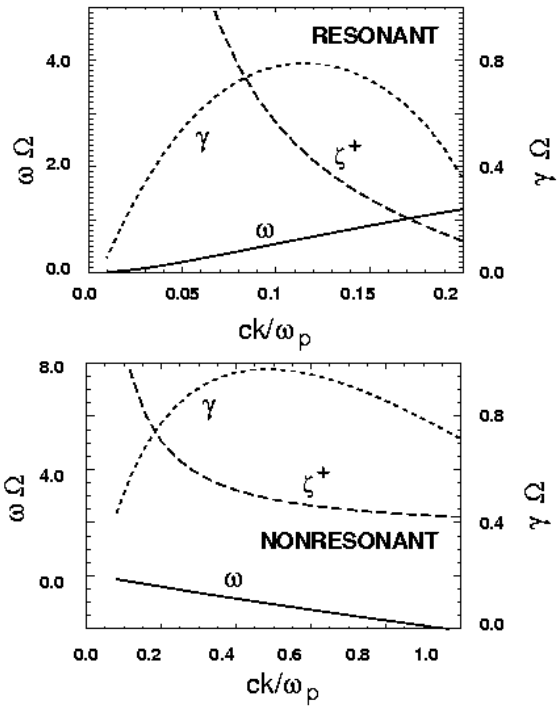

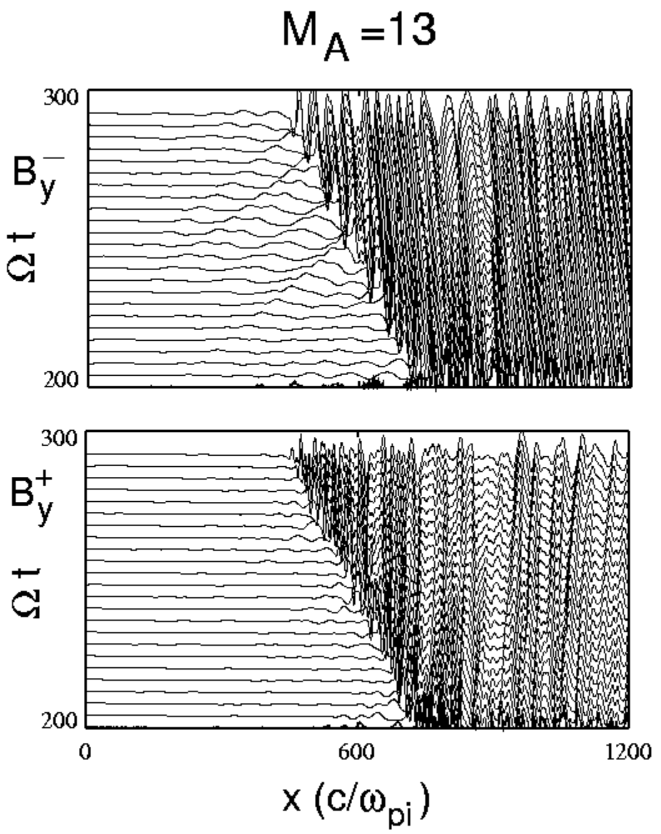

In high Mach number shocks the right hand resonant and right hand nonresonant instability are excited. The downstream turbulence is dominated by these large wavelength interface waves

(back to Parker and Golden et al.)

Scholer, Kucharek, Jayanti 1997

Short Large Amplitude Magnetic Structures SLAMSs and Shock Reformation

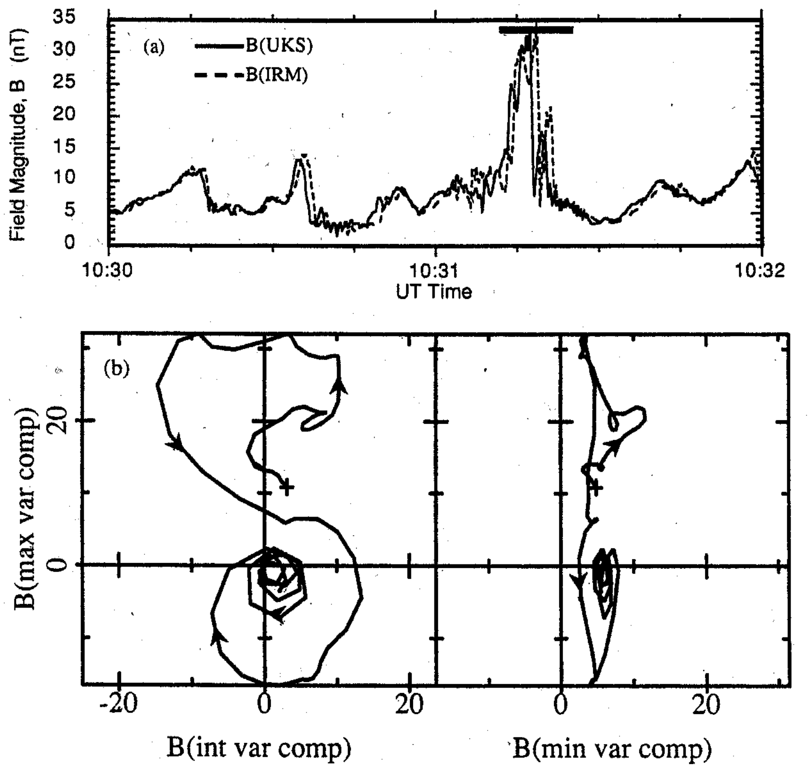

Oservations of SLAMSs at Earth‘s bow shock.
Top: temporal profile of magnetic
field magnitude; bottom: hodogram
In one SLAMS.

Schwartz et al. 1992

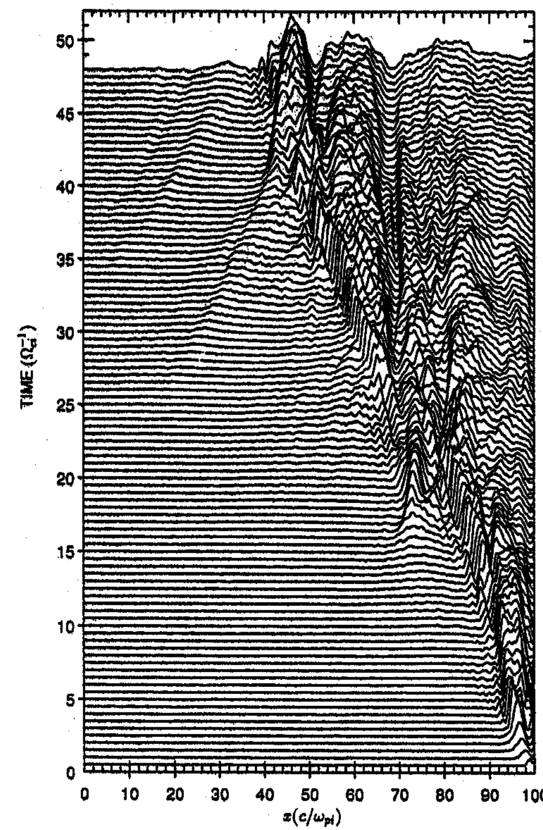

Hybrid simulation of a quasi-parallel shock showing shock reformation.

Burgess 1989

SLAMSs comprise the quasi-parallel shock

Upstream waves – interacion with diffuse ions –
SLAMSs – shock structure

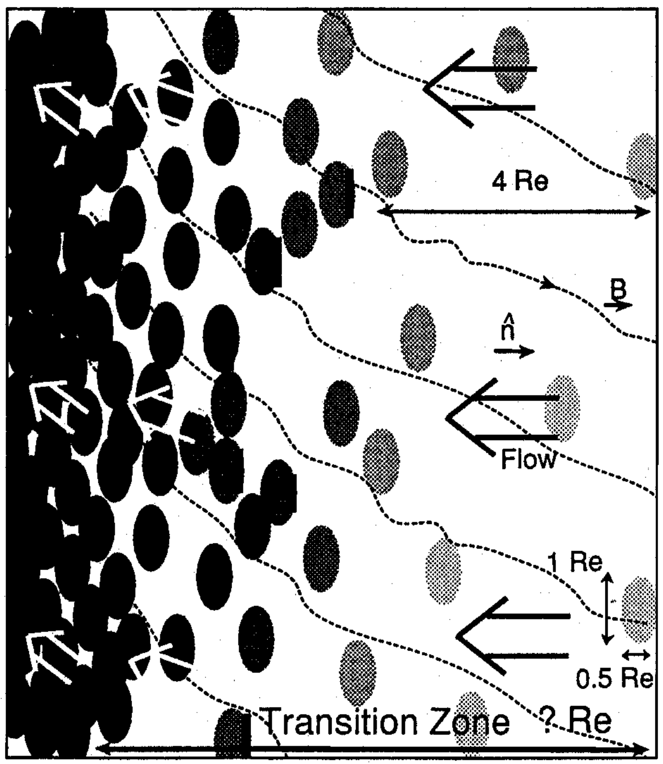

Schwartz and Burgess 1991

A collisionless quasi-parallel shock as due to formation, convection, growth, deceleration and merging of short large amplitude magnetic structures (SLAMSs).

SLAMSs have a finite transverse extent. Thus the shock is patchy when viewed, e.g., over the shock surface.

The downstream state is divided into plasma within SLAMSs and in inter-SLAMSs region.

Upstream Waves and Pulsations – 2-D

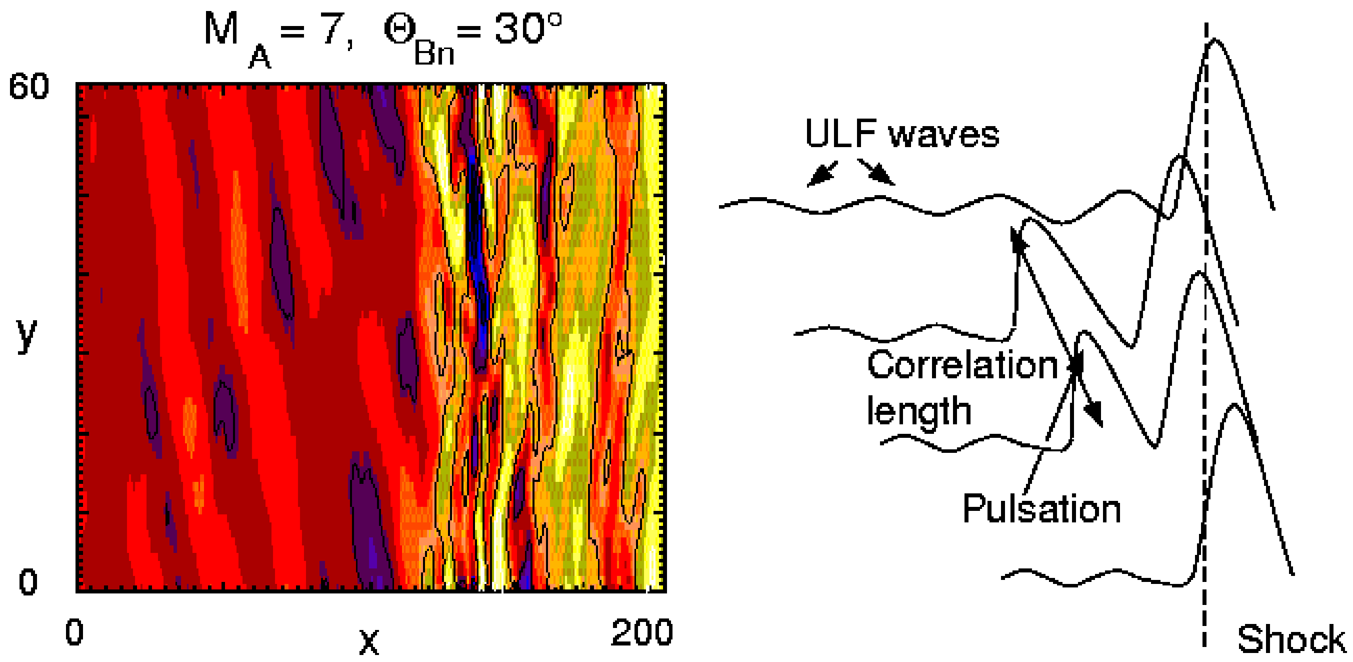

In 2-D k-vectors of upstream waves are aligned with magnetic field

When waves convect into region of increasing diffuse ion density they are refracted and wave fronts become aligned with shock front

Waves steepen and develop into large amplitude magnetic field pulsations

Scholer, Fujimoto, Kucharek 1997

Diffusive Acceleration

Simulation of a parallel shock in large-scale domain

Giacalone 2004

$M_A = 6.4$, $\beta = 1.5$

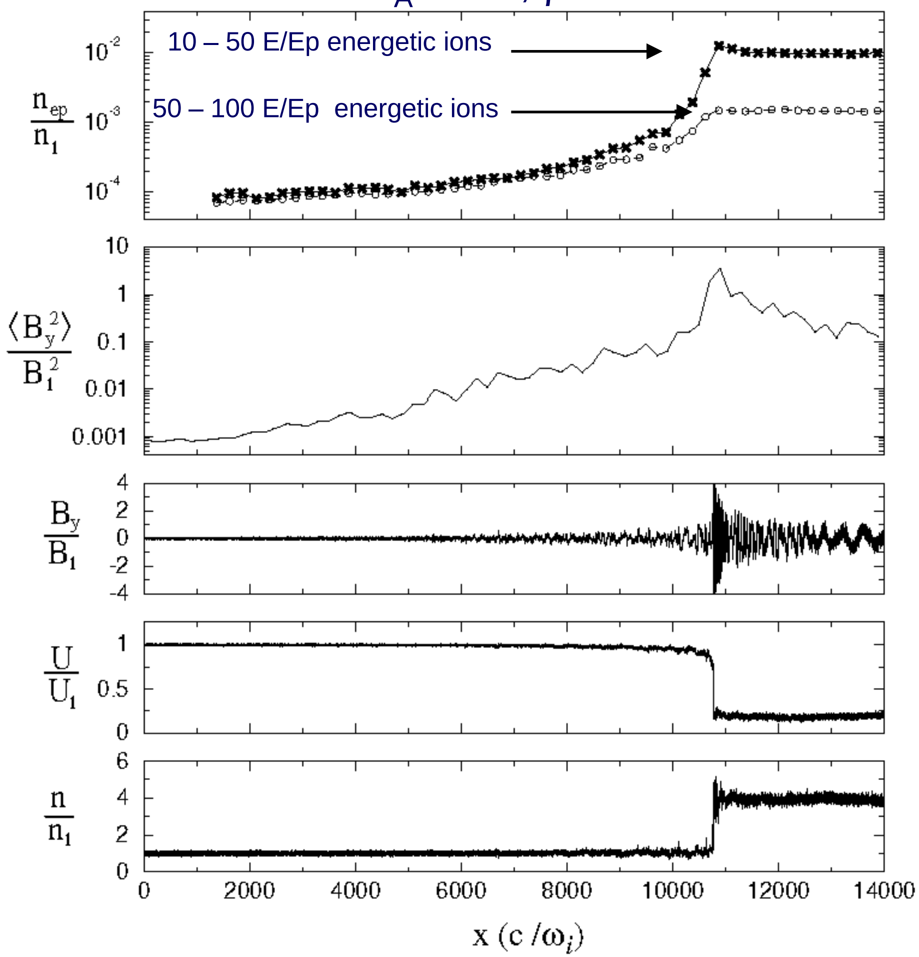

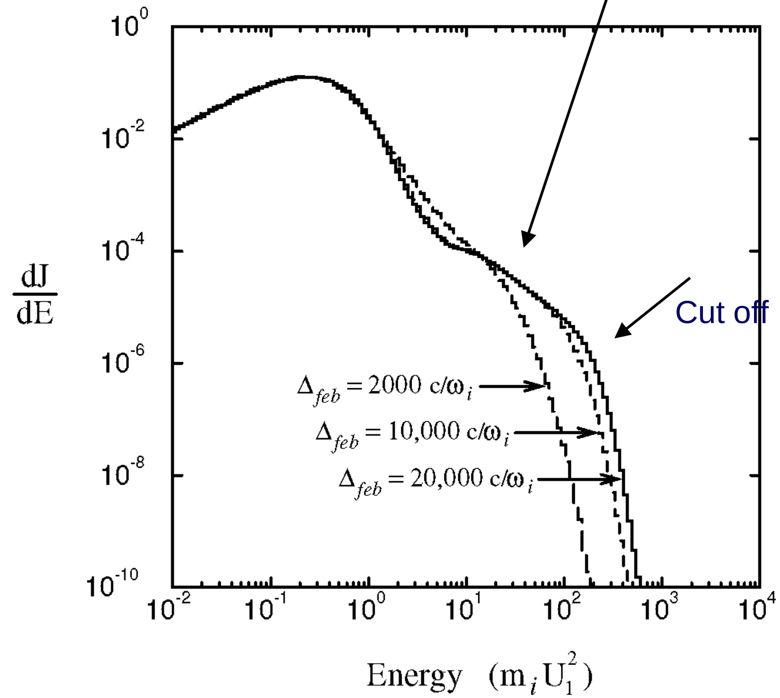

Downstream spectra for different distances from the free escape boundary. Cut-off energy much smaller than predicted by diffusive acceleration theory.

Injection

Trajectory of a typical solar wind proton trapped and accelerated at shock

Energy vs time.
red: tangential electric field is parallel to particle velocity,
blue: tangential electric field is antiparallel to velocity

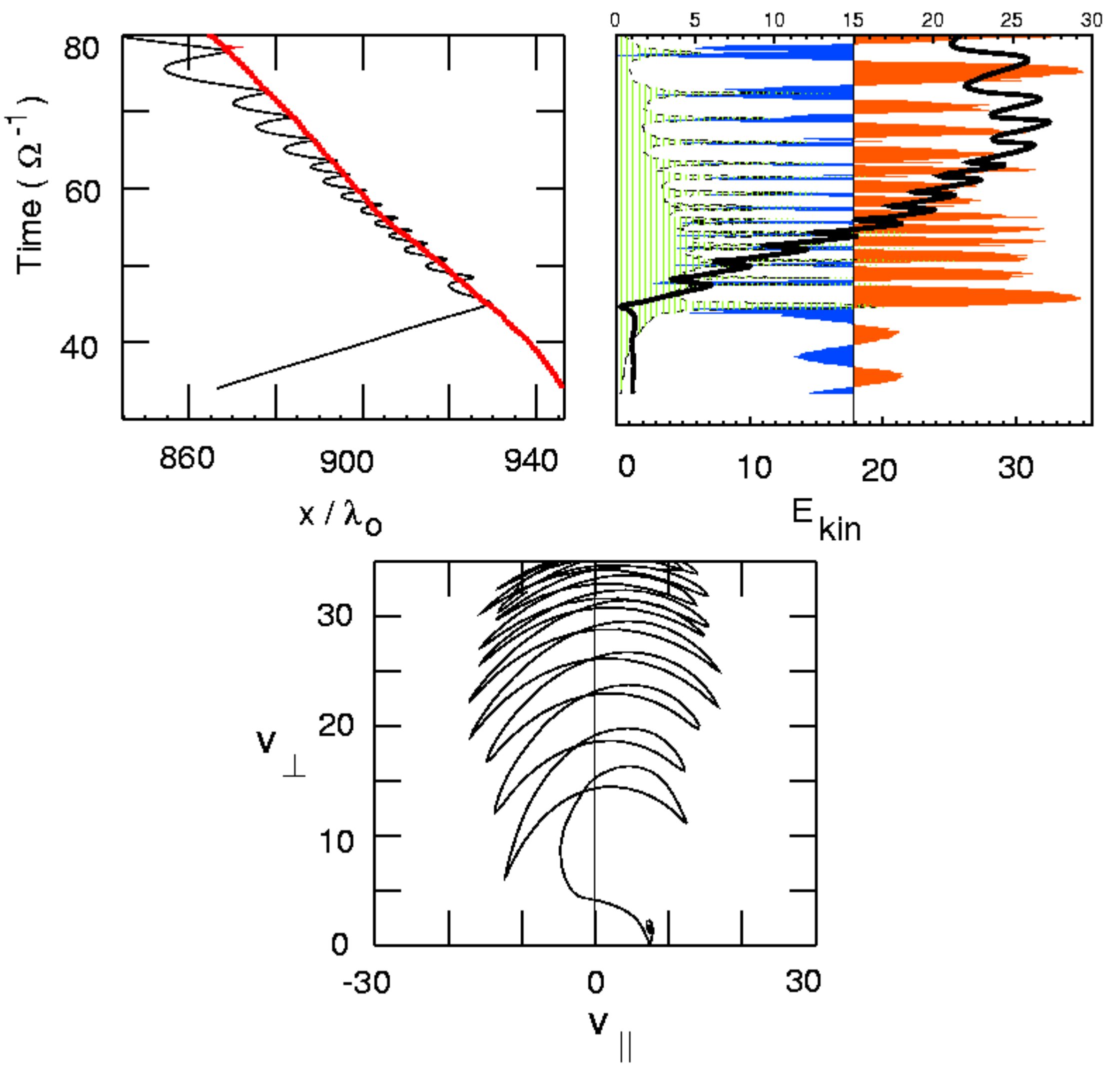

Trajectory in $v_\perp - v_\parallel$ space

Scholer et al. 2000

Nonlinear phase trapping in large amplitude monochromatic wave

Sugiyama and Terasawa 1999

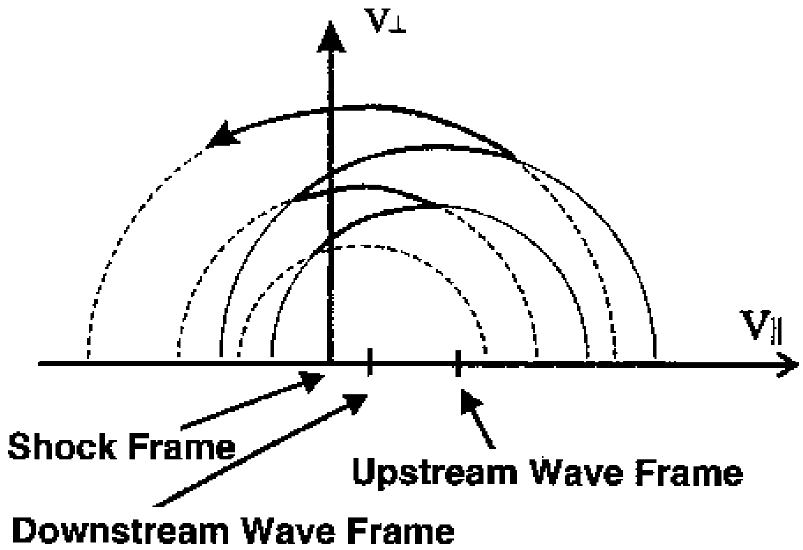

Ion is trapped between upstream and downstream wave train and gains energy

Parallel Shock Surfing

Krasnoselskikh et al. 2006

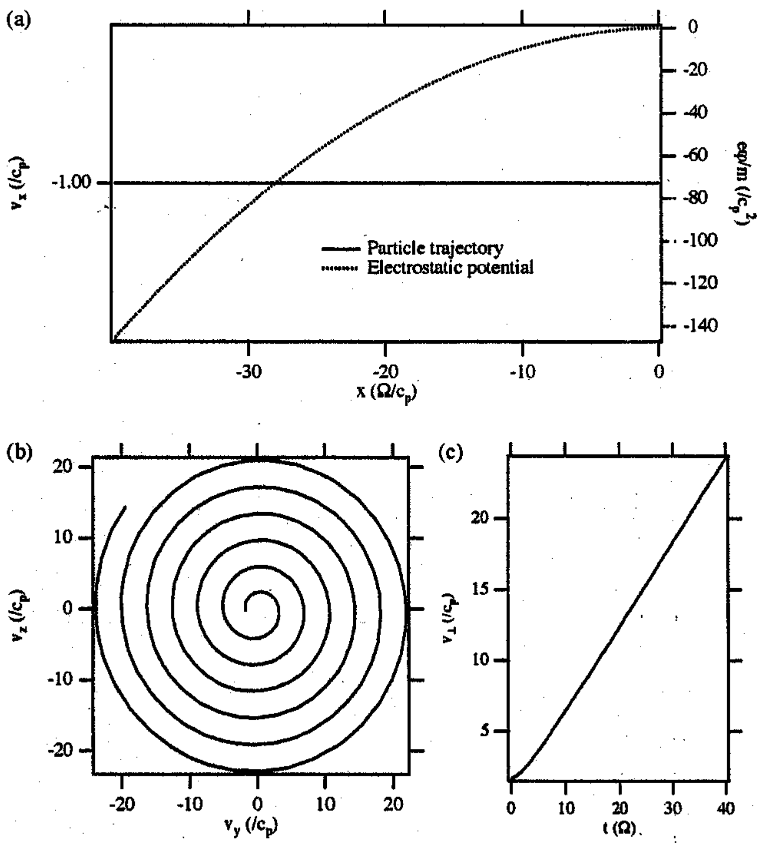

V x B force in x (shock normal) direction is at each point balanced by potential force so that the particle moves with constant velocity into the ramp

During this trajectory the particle is in cyclotron resonance with an upstream wave and gains perpendicular energy

Quasi-Perpendicular Collisionless Shocks

1. Specular reflection of part of incident ions

2. Downstream excitation of instabilities by temperature anisotropy

3. Rippling of shock surface

4. Shock reformation
   a) Upstream accumulation of reflected ions
   b) Instabilities in foot
   c) Nonlinear steepening of whistler or whistler triggered instability

5. Field Aligned Beams (FABs)

Schematic of Ion Reflection and Downstream Thermalization at Perpendicular Shocks

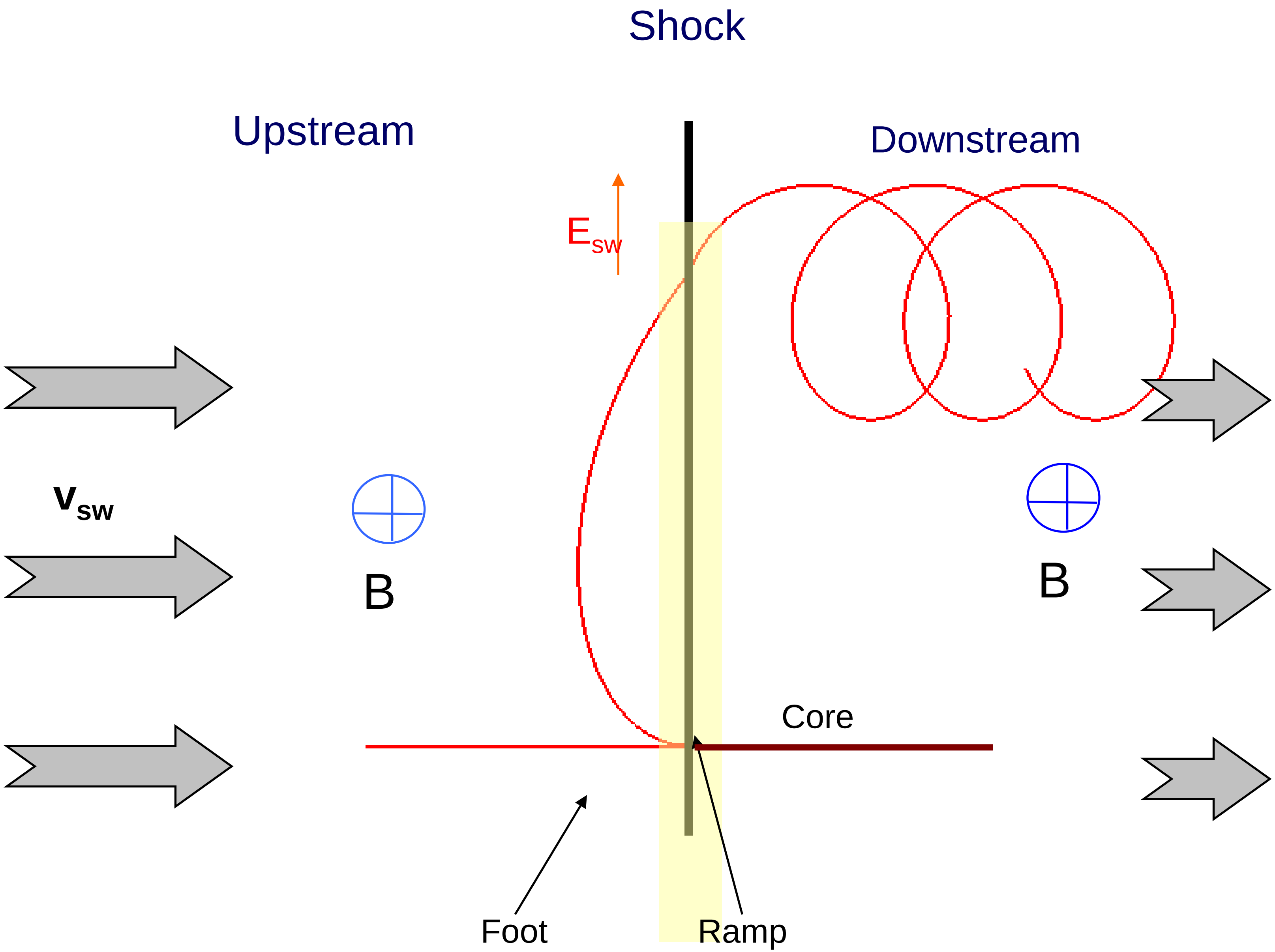

Specularly reflected ions in the foot of the quasi-perpendicular bow shock – in situ observations

Sckopke et al. 1983

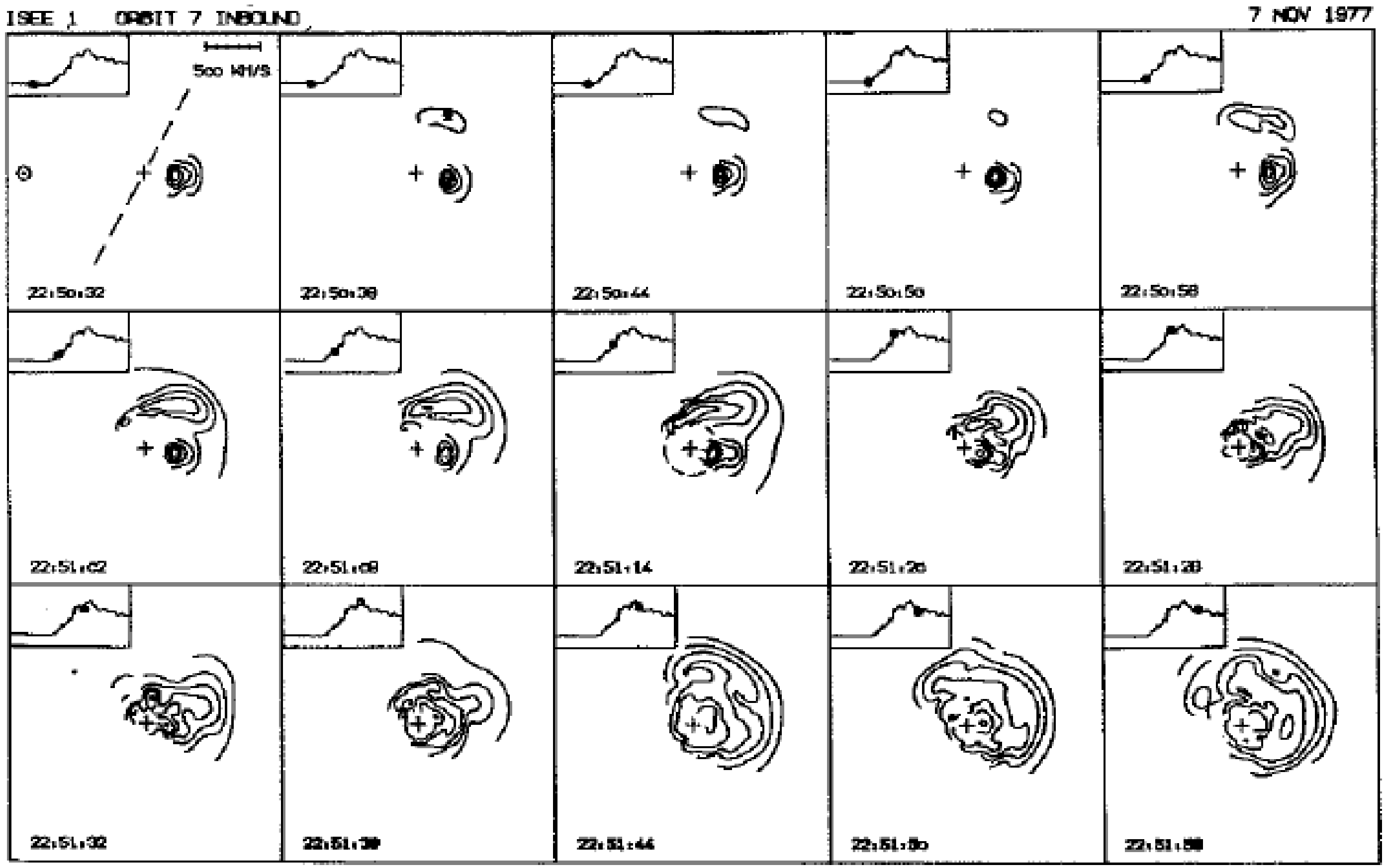

Ion velocity space distributions for an inbound bow shock crossing. The position of the measurement is shown by dots on the density profile. Phase space density is shown in the ecliptic plane with sunward flow to the left.

McKean, Omidi, Krauss-Varban 1995

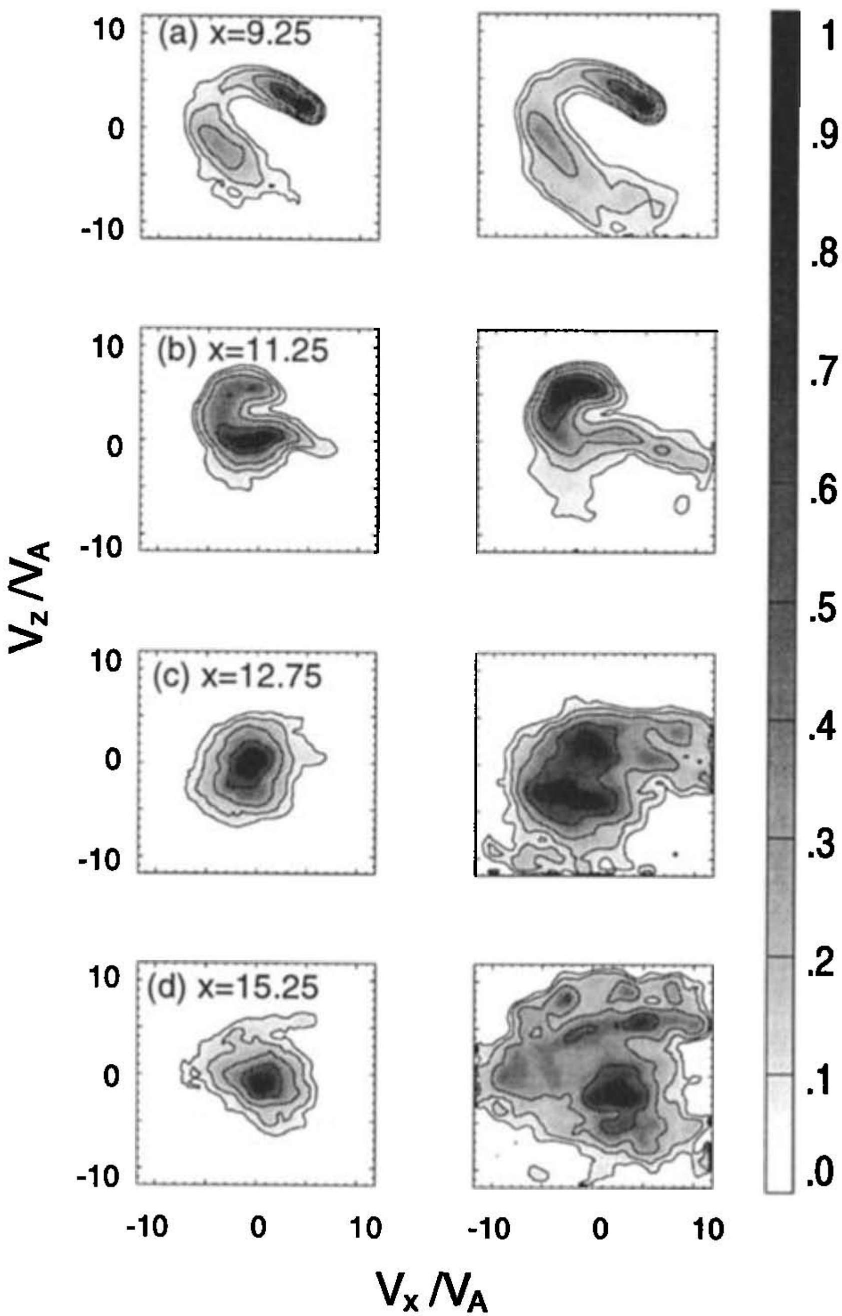

Iso-intensity contours of density (left) and energy density (right) in the plane perpendicular to the magnetic field going from upstream of he ramp (top) to downstream.

2-D Hybrid simulation of perendicular shock - B in simulation (x-y) plane

Winske and Quest 1988

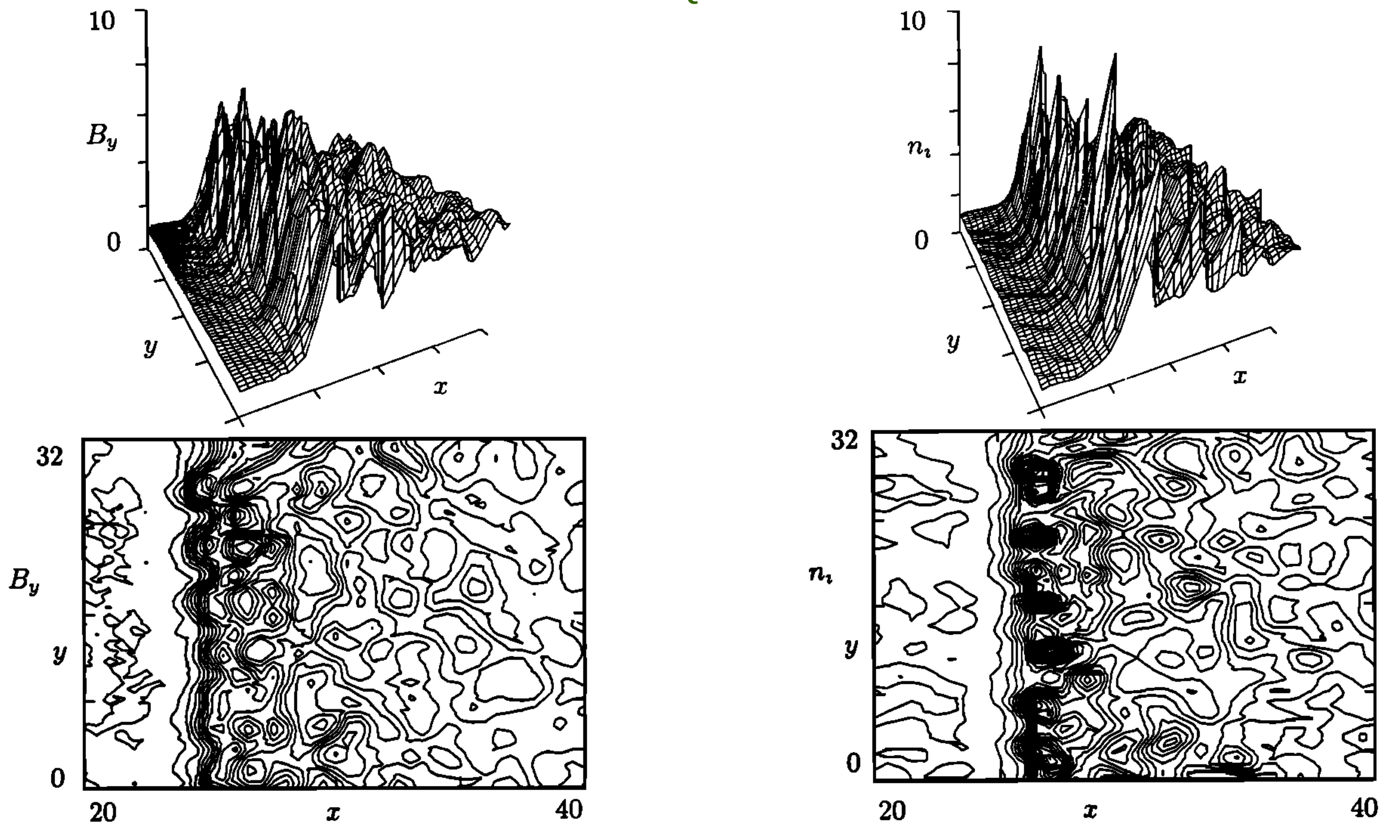

By magnetic field in x-y plane

Density in x-y plane

Oblique propagating Alfven Ion Cyclotron waves produced
by the perpendicular/parallel temperature anisotropy

Shock Ripples

Lowe and Burgess 2003

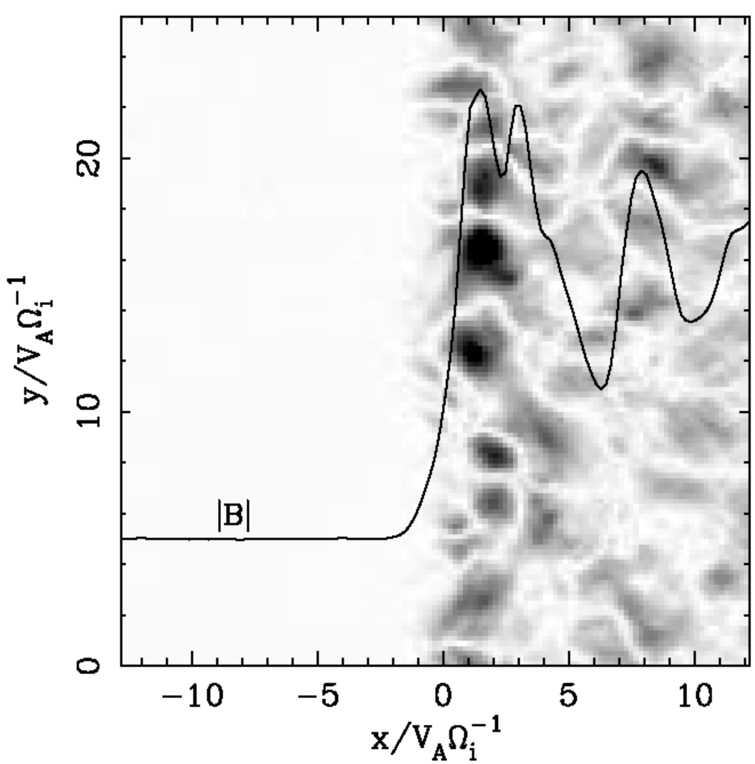

Burgess 2006

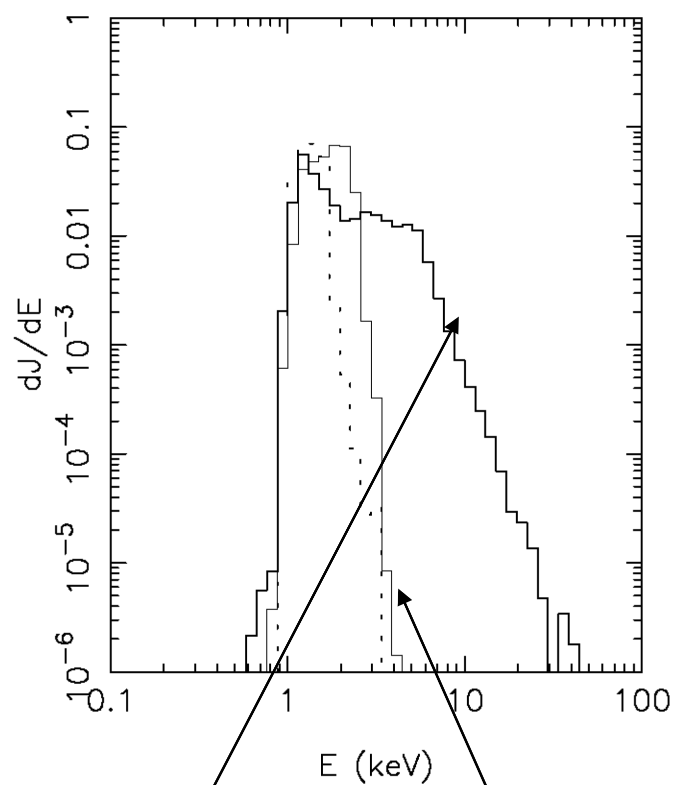

Ripples are surface waves on shock front
Move along shock surface with Alfven velocity given by magnetic field in overshoot

Electron acceleration (test particle electrons in hybrid code shock)

Shock with ripples

Shocks with no ripples

Instability due to specularly reflected ions

Burgess and Scholer 2006

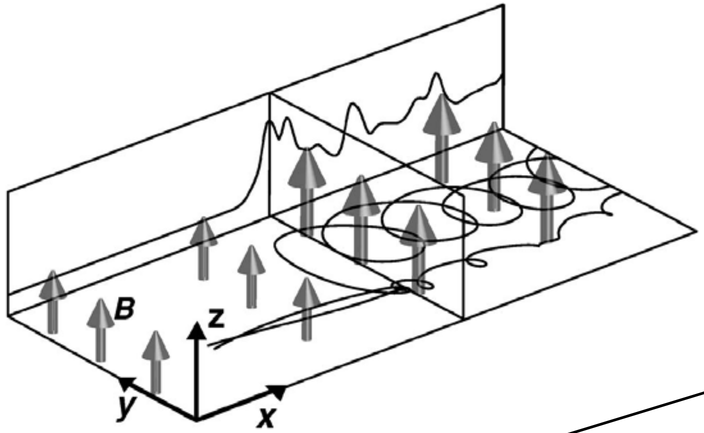

2-D simulation – magnetic field perpendicular to (x-y) simulation plane

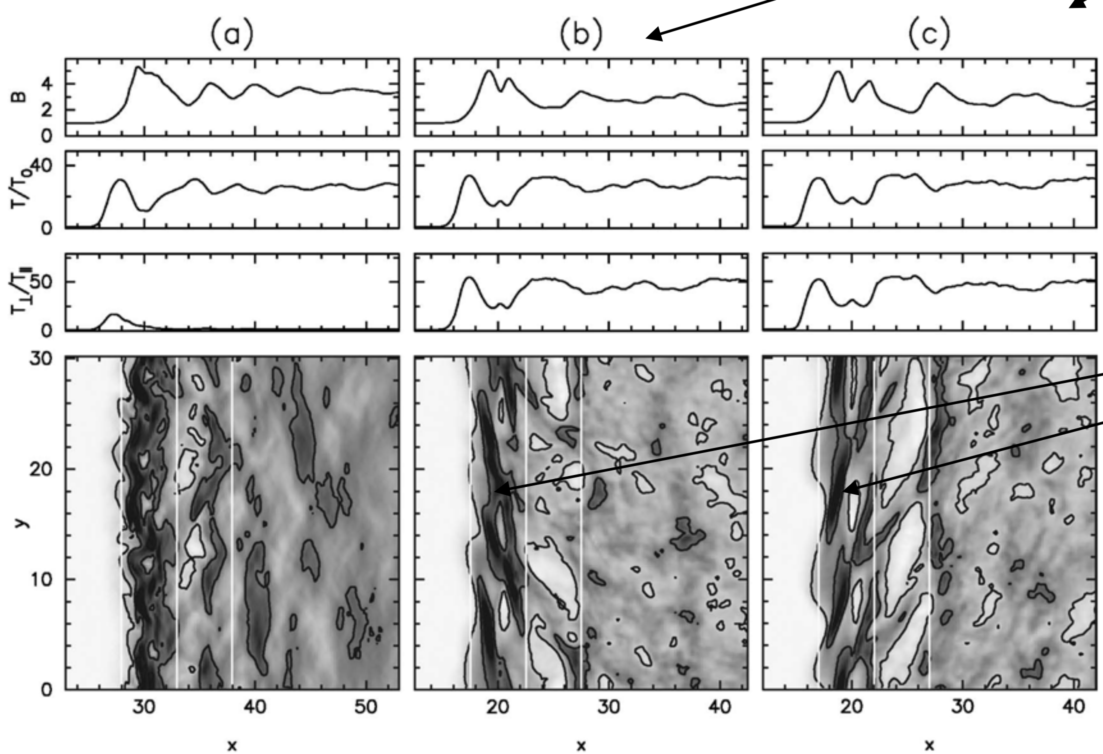

Ripples erpendicular to the magnetic field

Time evolution of the magnetic field in the ramp

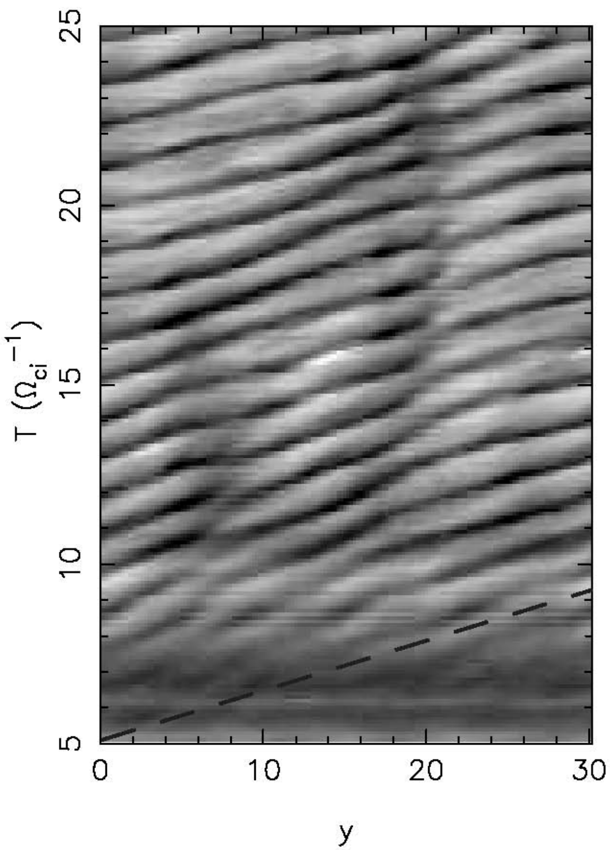

$\Theta_{Bz} = 0$

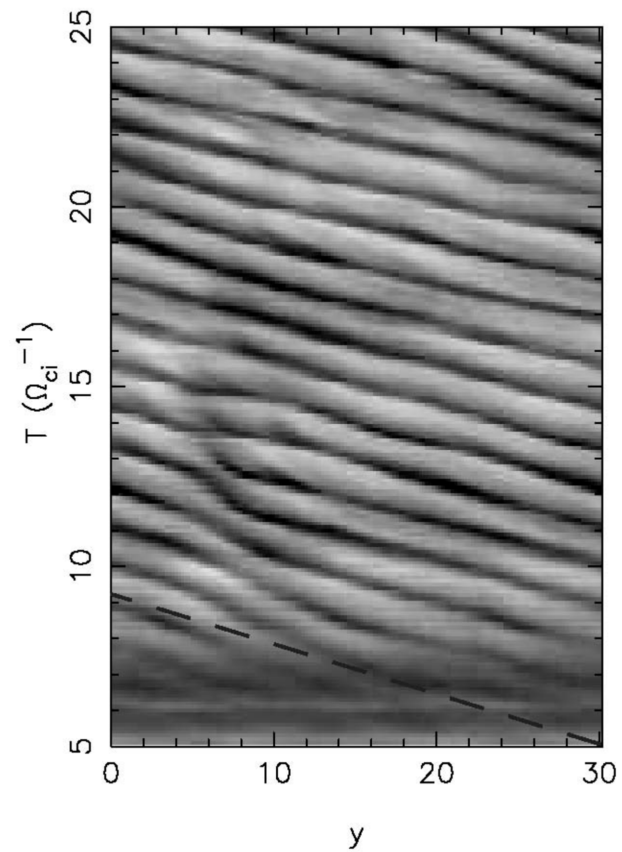

$\Theta_{Bz} = 180$

Pattern moves with constant speed along the shock
Sense of propagation is reversed when sense of magnetic field is reversed
Speed of pattern is the same as average y velocity of specularly reflected ions
Sense of propagation is same as gyromotion of reflected ions

Self-Reformation of Quasi-PerpendicularShocks

1. Self-reformation by ion accumulation

Hada, Oonishi, Lembege, Savoini 2003

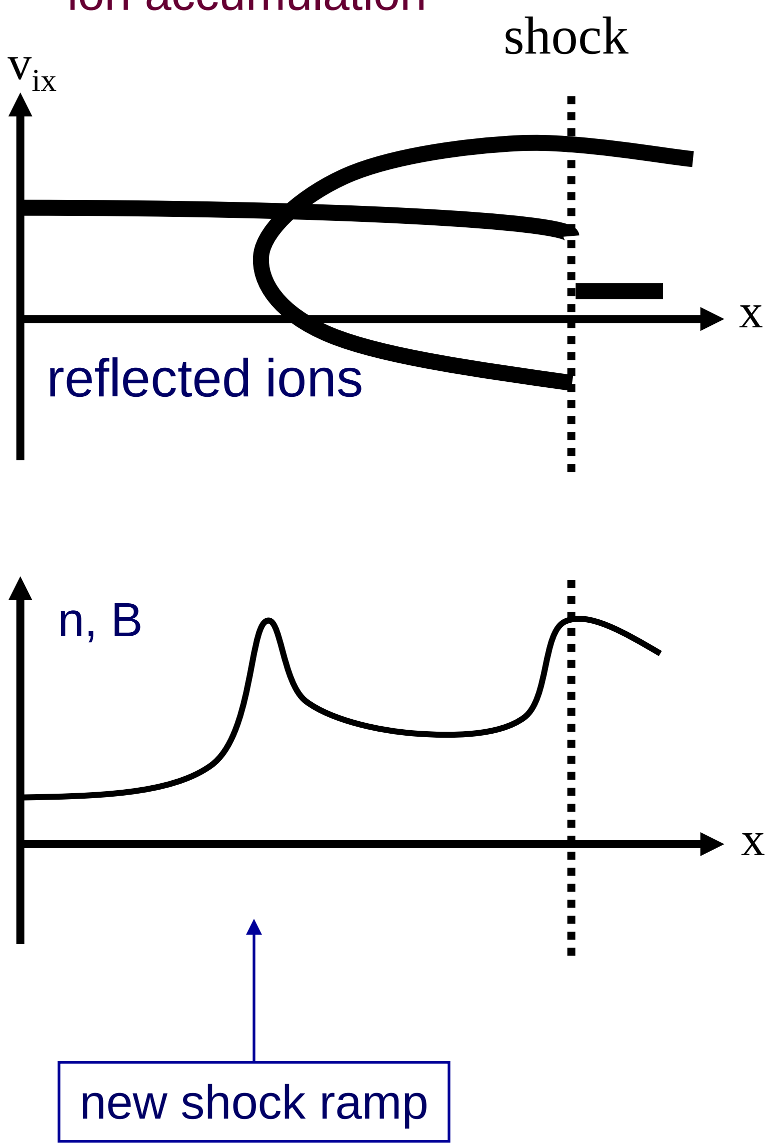

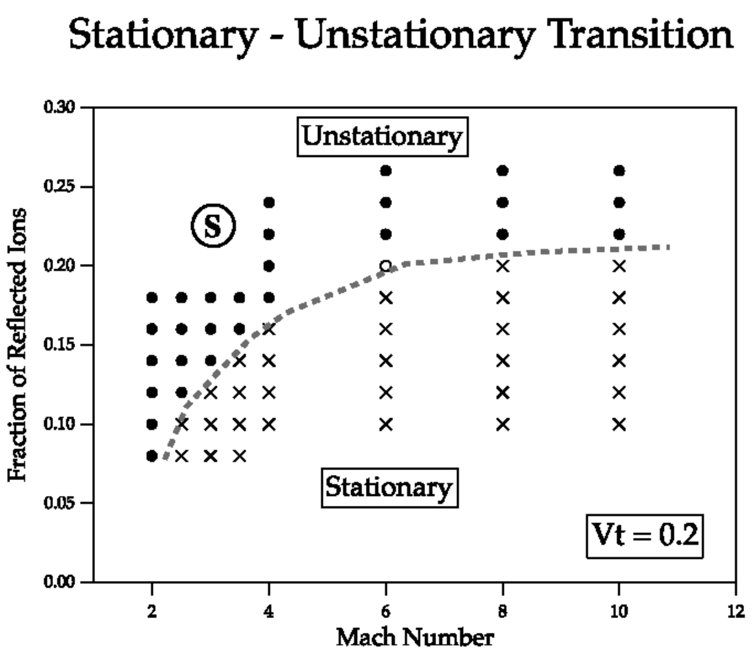

Situation in the foot region of a perpendicular shock

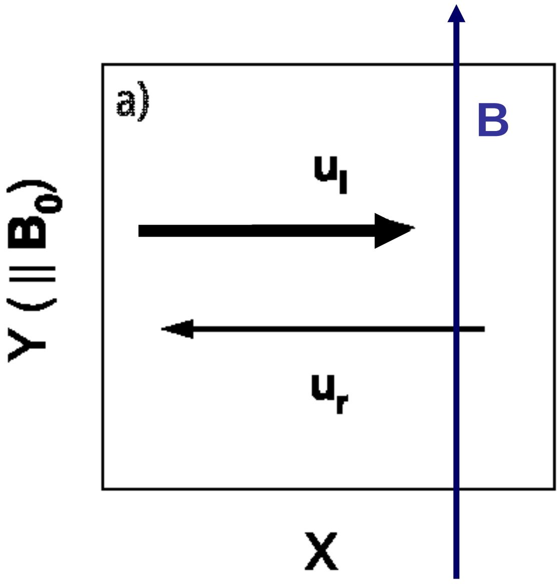

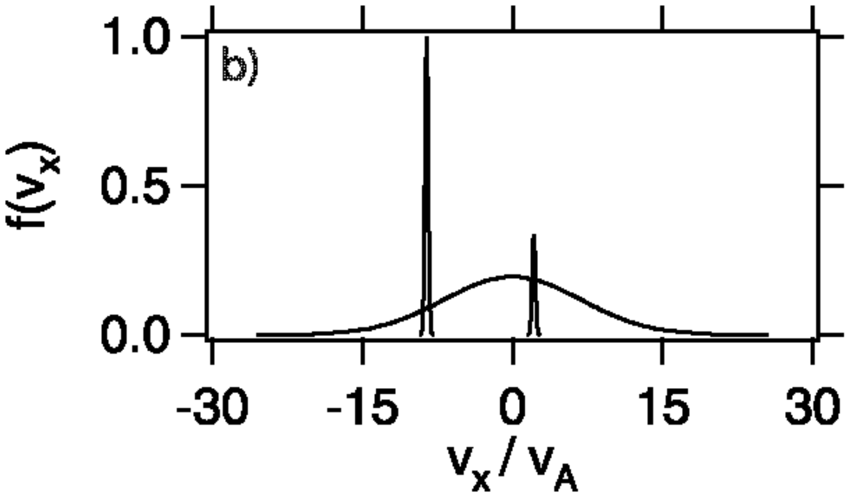

Ion and electron distributions in the foot

Ions: unmagnetized
Electrons: magnetized

2. Micro-Instabilities in the foot

Scholer, Shinohara, Matsukiyo 2003

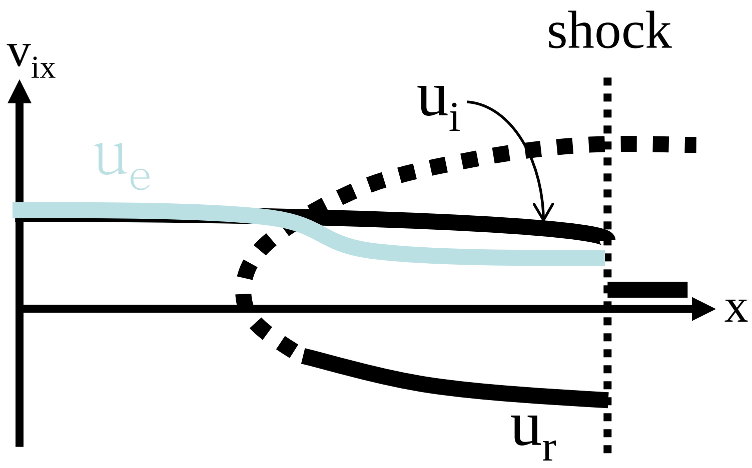

Source of instabilities

$$u_r \neq u_e$$

$$u_i \neq u_e$$

Possible microinstabilities in the foot

	Wave type	Necessary condition
Buneman inst.	Upper hybrid (Langmuir)	$\Delta u >> v_{te}$
Ion acoustic inst.	Ion acoustic	$T_e >> T_i$
Bernstein inst.	Cyclotron harmonics	$\Delta u > v_{te}$
Modified two-stream inst.	Oblique whistler	$\Delta u/\cos\theta > v_{te}$

Linear Properties of the Modified Two-Stream Instability

(Between incoming ions and incoming electrons
the foot of a quasi-perpendicular shock)

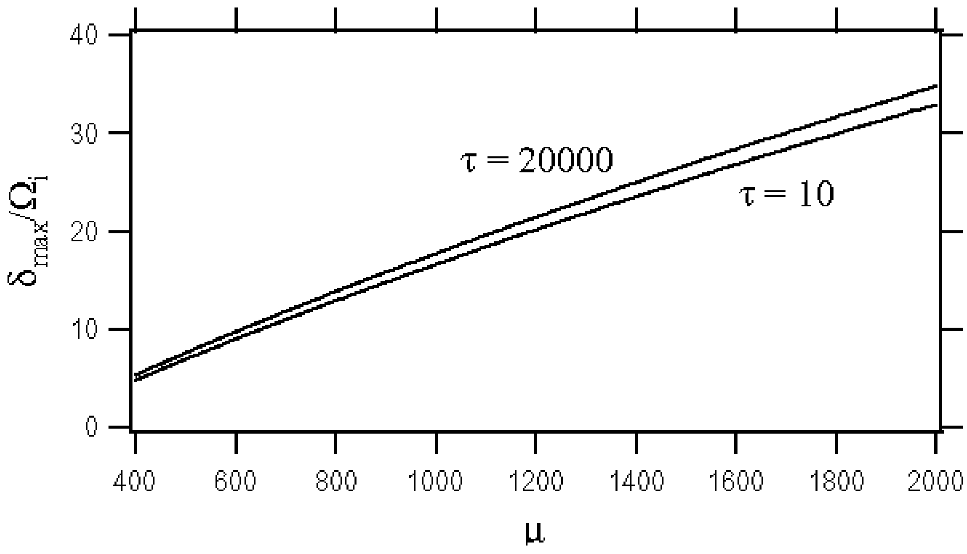

$\tau = (\omega_{pe} / \omega_{ce})^2$

Maximum growth rate (normalized to ion gyrofrequency) for cold plasma as a functon of ion to electron mass ratio μ

Matsukiyo and Scholer 2003

Parameters in PIC Simulations of Collsionless Shocks

1. Mass ratio m_i / m_e

2. Ratio of electron plasma to gyrofrequency $$\nu = \frac{\omega_{pe}}{\Omega_{ce}} = \frac{c}{V_A}\sqrt{\frac{m_e}{m_i}}$$

	m_i / m_e	$\omega_{pe} / \omega_{ce}$		c / V_A
Solar Wind	1836	100 – 200		(5000)
Biskamp and Welter, 1973	124	5	1-D	
Lembege and Dawson, 1987	100	2	1-D	
Liewer et al., 1991	1836	1-4	1-D	
Savoini and Lembege, 1994	42	2	2-D	
Shimada and Hoshino, 2000,2003,2005	20	20	1-D	(90)
Lembege and Savoini, 2002	42	2	2-D	
Krasnoselskikh et al., 2002	200	-	1-D	
Hada, Oonishi. Lembege, Savoini 2003	84	2	1-D	(18)
Scholer, Shinohara, Matsukiyo, 2003	1840	2	1-D	(95)
Scholer, Matsukiyo, 2004	1840	2	1-D	
Muschietti and Lembege, 2005	100	2	1-D	(20)
Matsukiyo, Scholer, 2006	1860	2	2-D	
Scholer, Comisel, Matsukiyo, 2007	1000	5	1-D	(150)

Reformation of almost perpendicular medium Mach number shocks: Mass ratio and ion beta effect

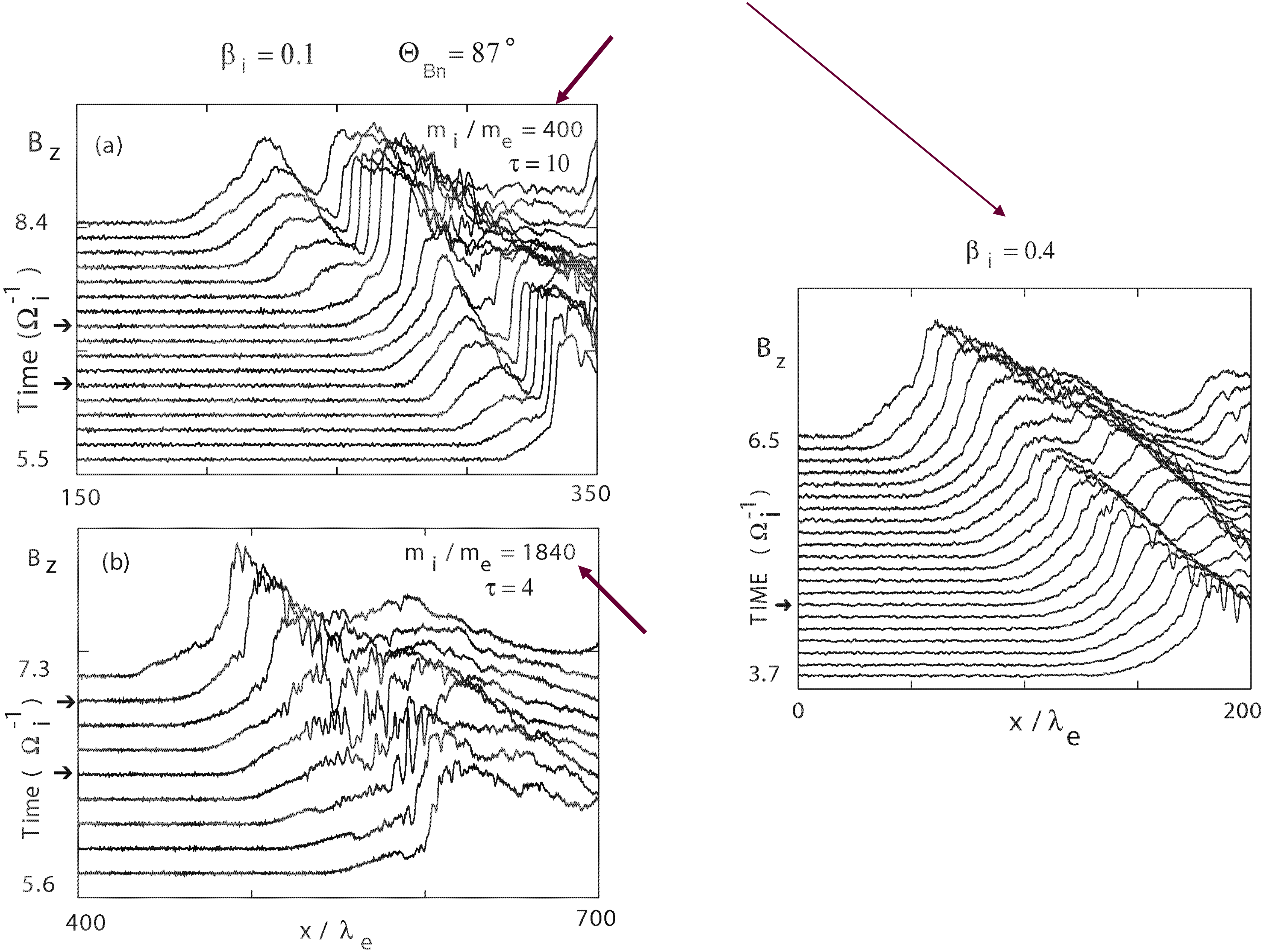

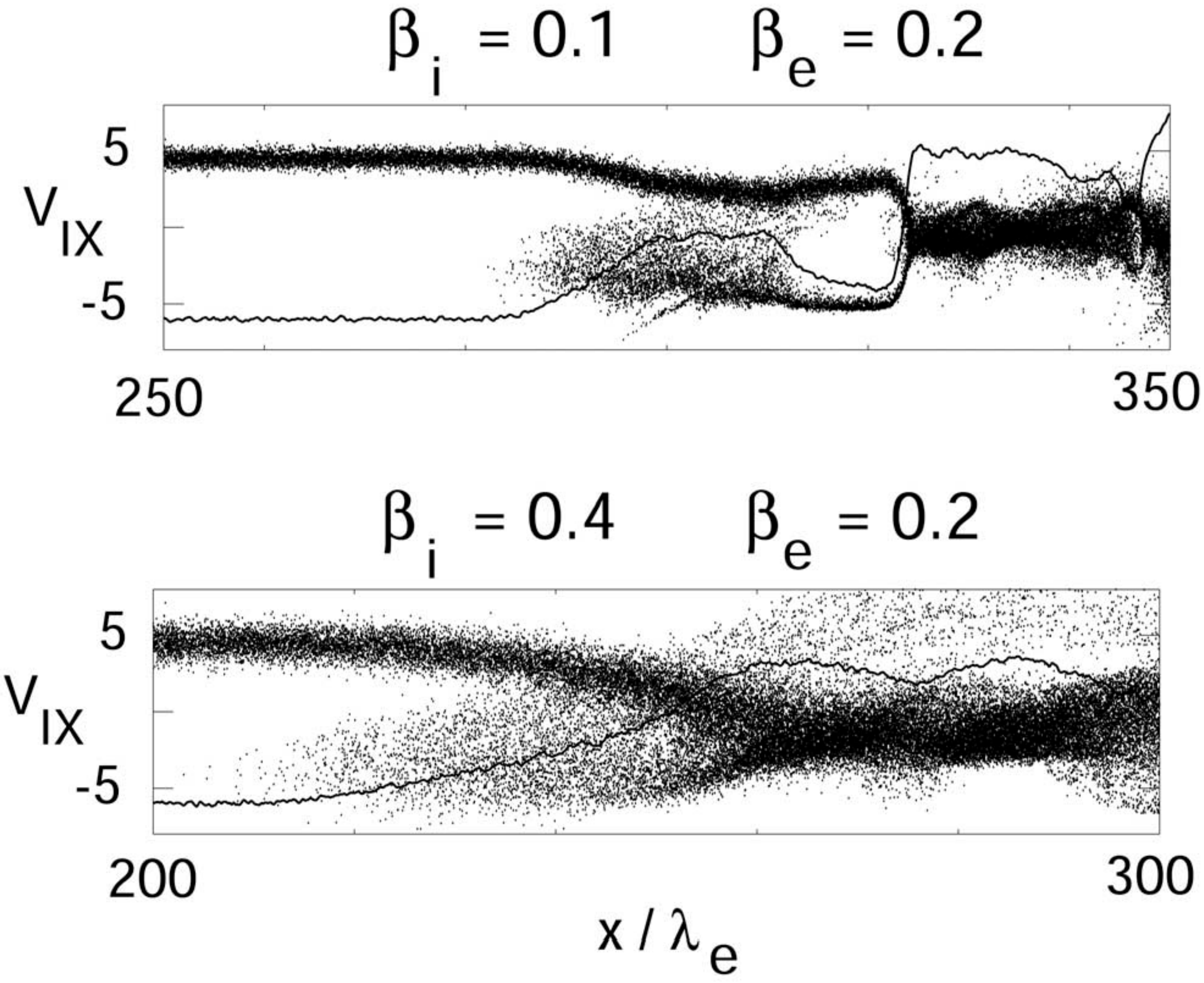

Self-reformation is a high (ion) beta mechanism. More precise: velocity difference between reflected and incoming ions has to be larger than ion thermal velocity.

$$\beta_i = \beta_e = 0.05$$

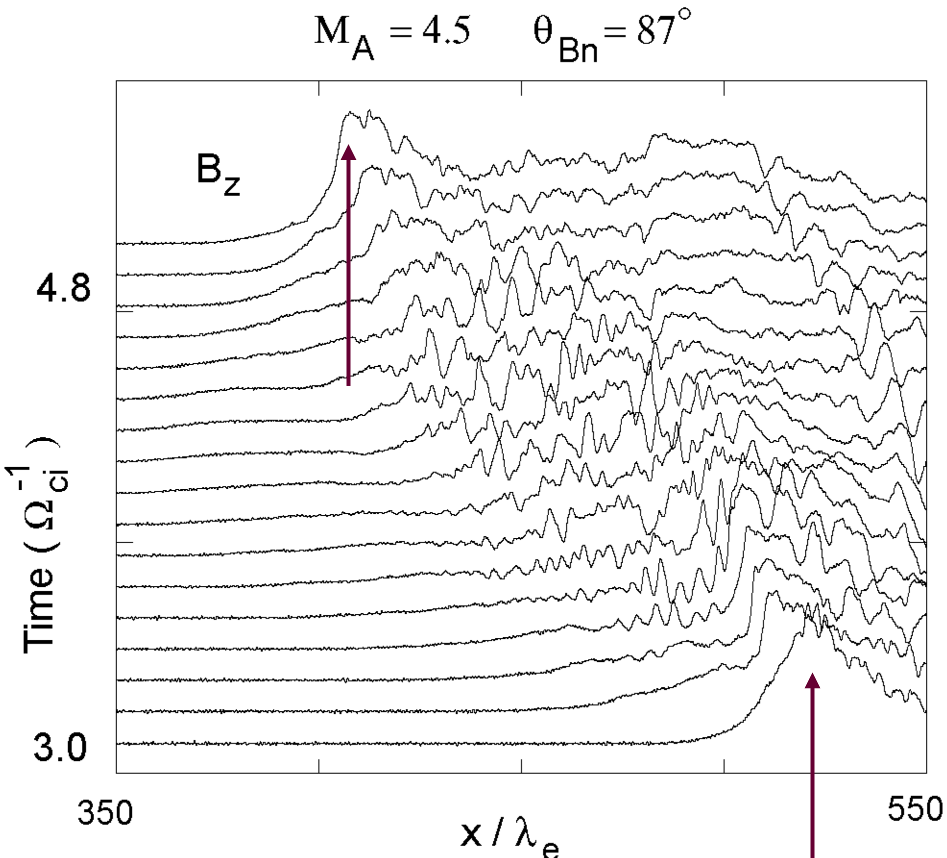

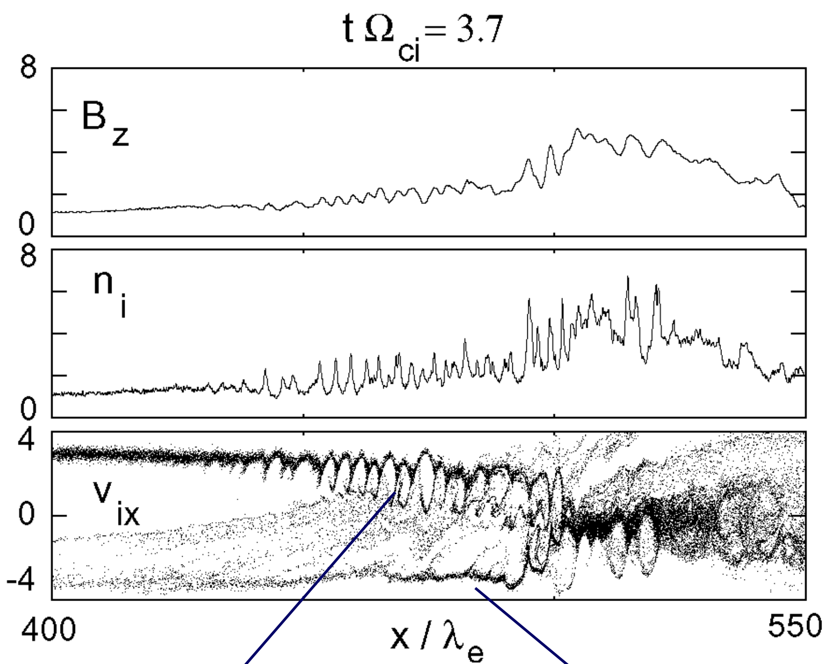

Instability between incoming ions and incoming electrons leads to perpendicular ion trapping

Reflected ions not effected

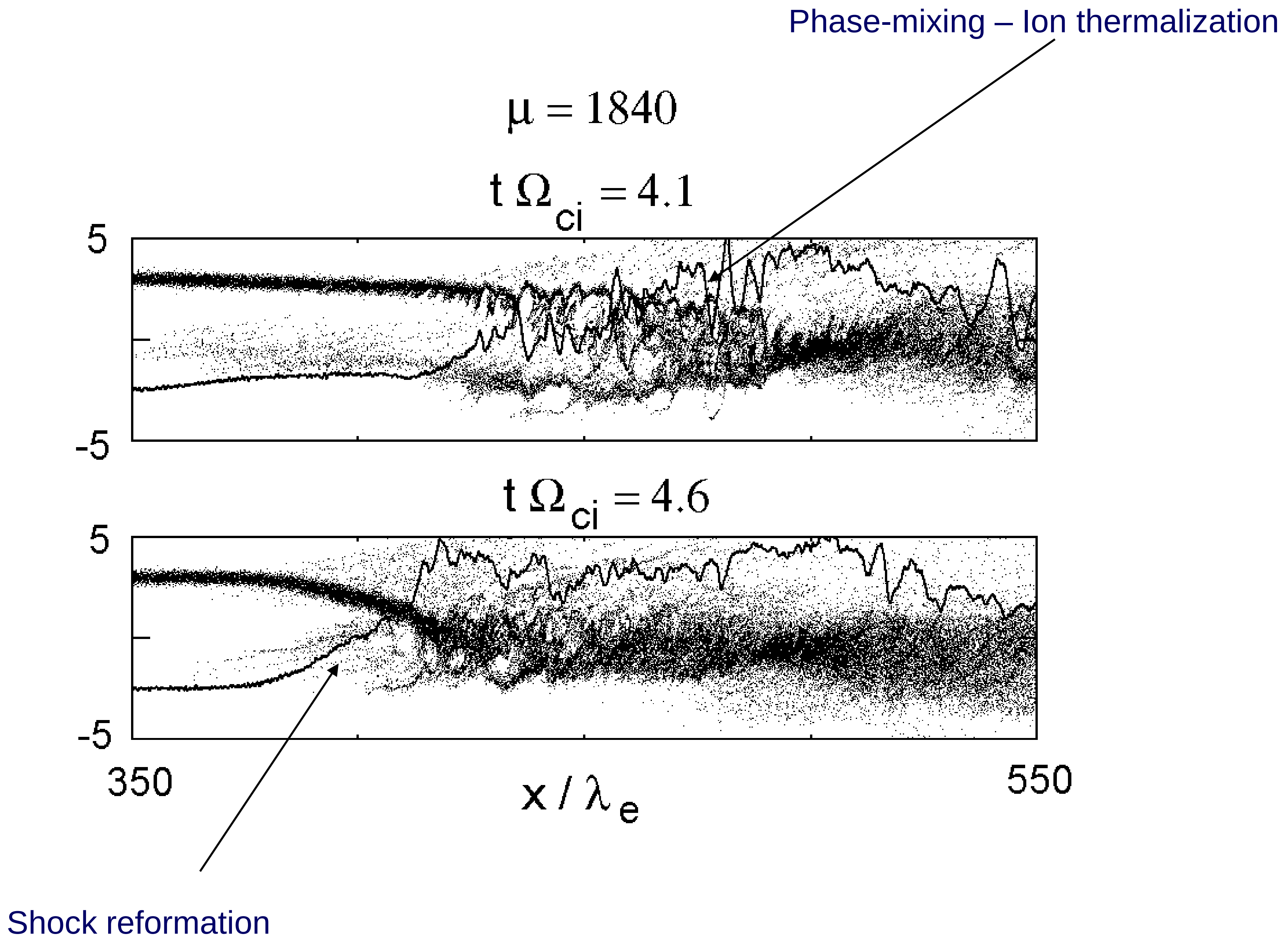

Phase-mixing – Ion thermalization
μ = 1840
t Ω ci = 4.1
5
-5
t Ω ci = 4.6
5
-5
350
550
x / λ e
Shock reformation

Modified Two-Stream Instability (MTSI)

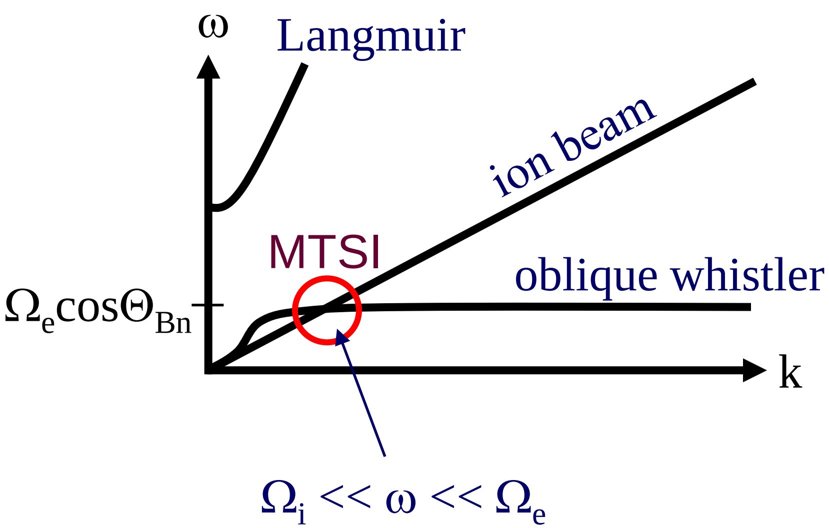

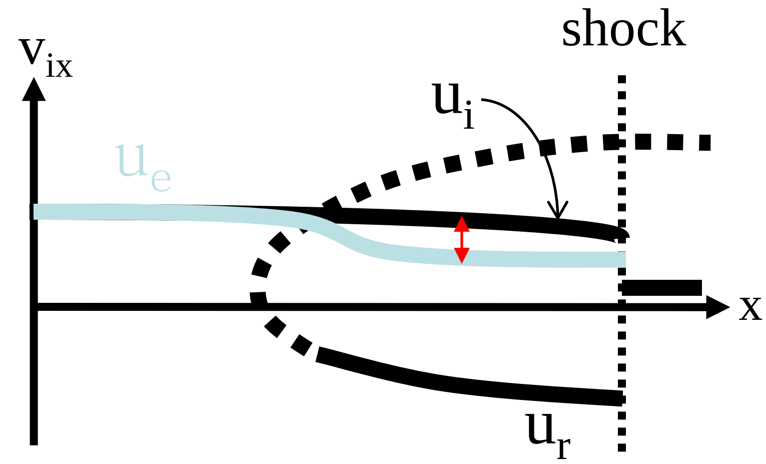

unmagnetized ions ⟶ perpendicular trapping

strongly magnetized electrons ⟶ parallel trapping

3. Gradient catastrophe of nonlinear upstream whistler at oblique shocks

Krasnoselskikh et al. 2002

Whistler critical Mach number

$$M_w = \frac{|\cos\Theta_{Bn}|}{2(m_e/m_i)^{1/2}}$$

Below M_w exists phase standing small amplitude upstream whistler

Nonlinear whistler critical Mach number

$$M_{nw} = \frac{|\cos\Theta_{Bn}|}{(2m_e/m_i)^{1/2}}$$

Above M_{nw} shock nonlinear steepening of waves can not be canceled anymore by dispersion and/or dissipation and becomes non-stationary

4. Nonlinear instability beween incoming solar wind and reflected ions

Biskamp and Welter 1972

Incoming and reflected ion beams are stable if velocity difference large (note: ions are unmagnetized)

A nonlinear beam-instability between incoming and reflected ions is then triggered by the electric field of the large amplitude upstream whistler

Biskamp and Welter 1972

(PIC simulation 36 years ago!)

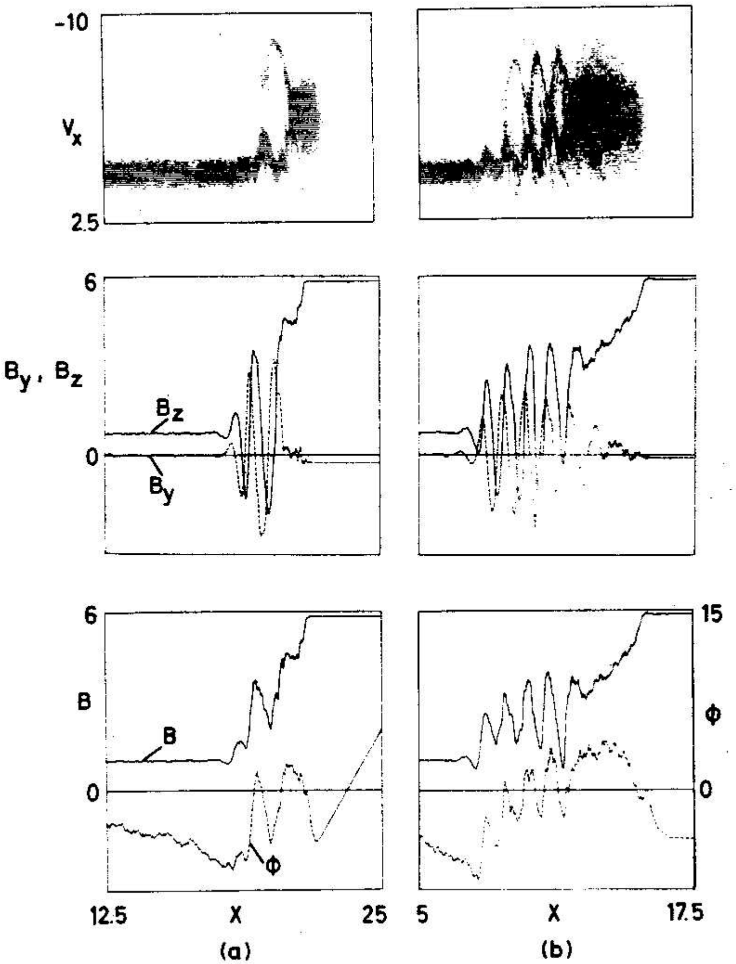

Fig. 2. Ion phase space x and v_x, magnetic field components B_y and B_z, total magnetic field B, and electric potential ϕ of a magnetic shock at (a) $t = 1.25/\Omega_i$ and (b) $t = 3.25/\Omega_i$. The mass ratio is $m_i/m_e = 128$.

$M_A = 5.0$

Small mass ratio, but also small Θ_{Bn} of 45^o, therefore M_w reasonable large, i.e., were able to Investigate influence of reflecetd ions

45

$$M_w = \frac{|\cos\Theta_{Bn}|}{2(m_e/m_i)^{1/2}} = 4.0$$

Buneman Instability

Strongly suppressed by Landau damping when relative drift between electrons and reflected ions smaller than electron thermal velocity.

$$V_{r-e} > \sqrt{2} v_{the}$$

$$v_{the} / V_A = \sqrt{(0.5\beta_e)(m_i / m_e)}$$

We assume that the reflected ions have the same velocity as the incoming ions
And that the incoming electrons are decelerated in order to achieve zero electrical current in the normal direction. The Buneman instability is stabilized if

$$\beta_e \geq 4 M_A^2 (1+\alpha)^2 (m_e / m_i)$$

where α denotes density ratio of reflected and incoming ions

With m_i/m_e=1840, $\alpha=0.25$, the Buneman instability can not grow unless

$$\beta_e \lesssim M_A^2 / 720$$

Buneman instability only at large Mach number or small electron beta

Importance of Buneman Instability for Electron Acceleration In High Mach Number Shocks

Shimada and Hoshino 2003

$$\Theta_{Bn} = 90^\circ, M_A = 11$$

$$m_i / m_e = 20, \beta_i = \beta_e = 0.5, \omega_{pe} / \Omega_{ce} = 20$$

Nonlinear state of the Buneman instability – Electron holes

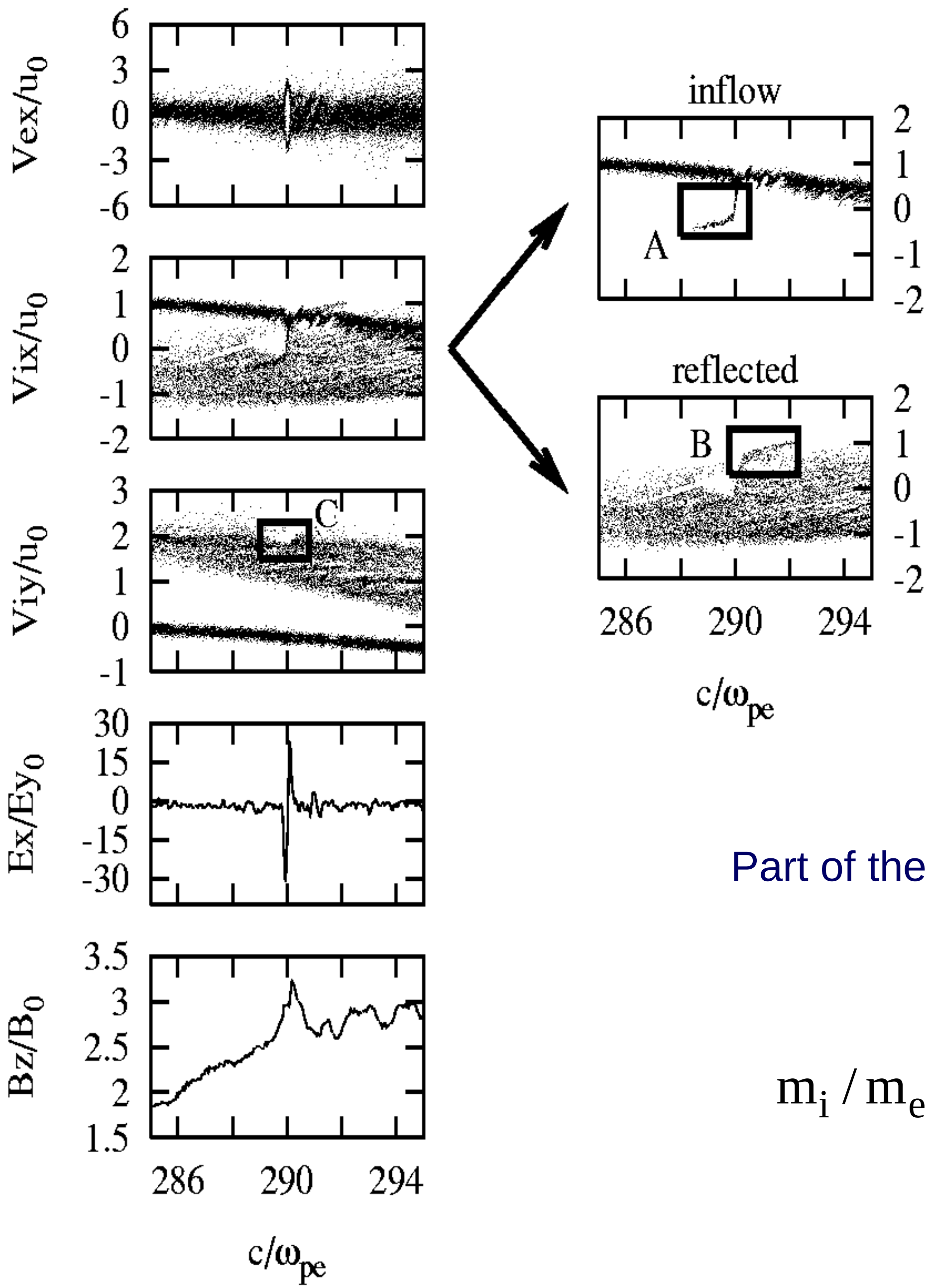

Part of the shock transition region with electron hole

$$\Theta_{Bn} = 90^\circ, M_A = 11$$

$$m_i / m_e = 20, \beta_i = \beta_e = 0.5, \omega_{pe} / \Omega_{ce} = 20$$

Shimada and Hoshino 2003

Electron hole generation by nonlinear development of Buneman instability
Large-amplitude electron hole couples to ions via ion acoustic fluctuations.
Decelerates incoming and reflected ions and leads to further potential increase in the hole.

Hole disappears and electrons are heated and accelerated

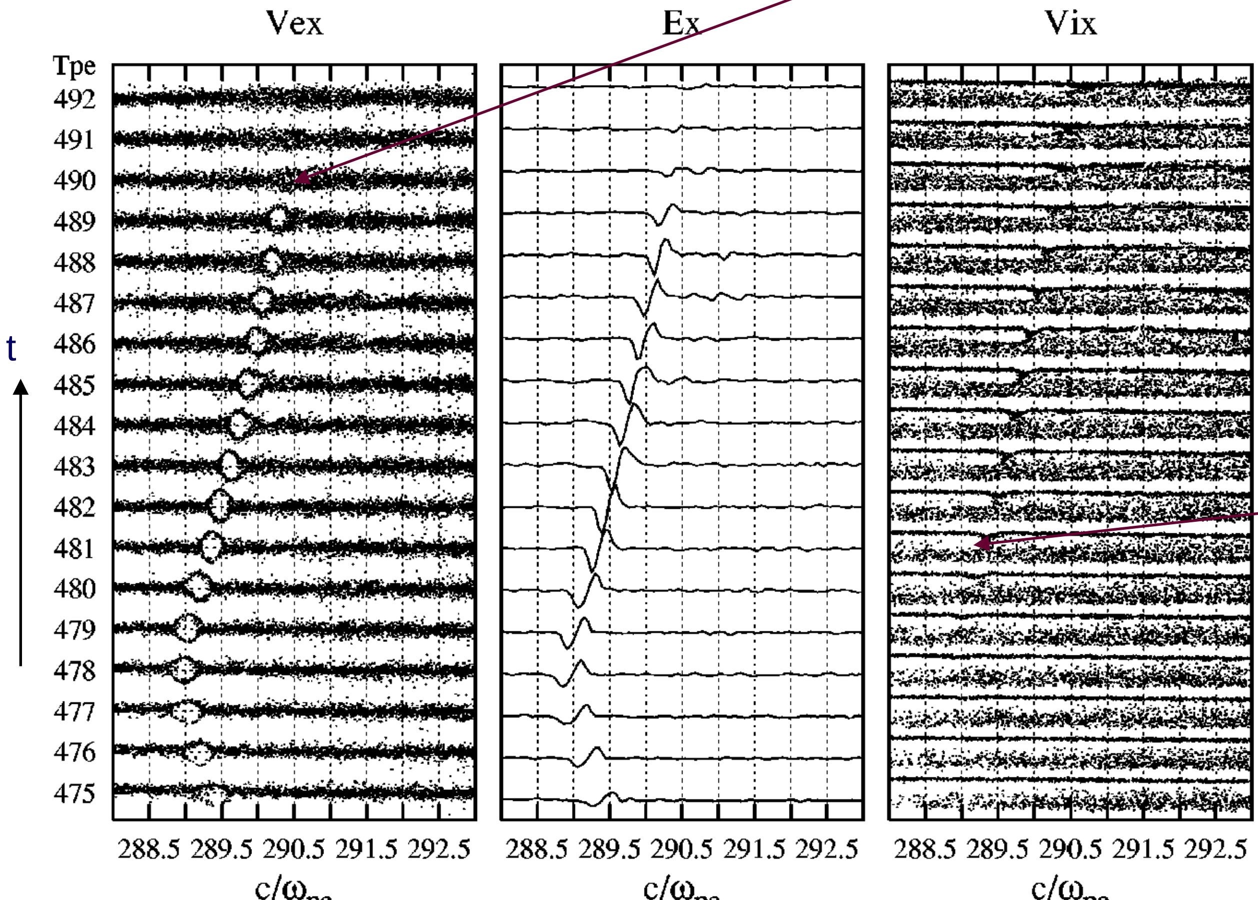

Coupling of hole to the incoming ions

Field-Aligned Beams (FABs) at the Quasi-Perpendicular Shock

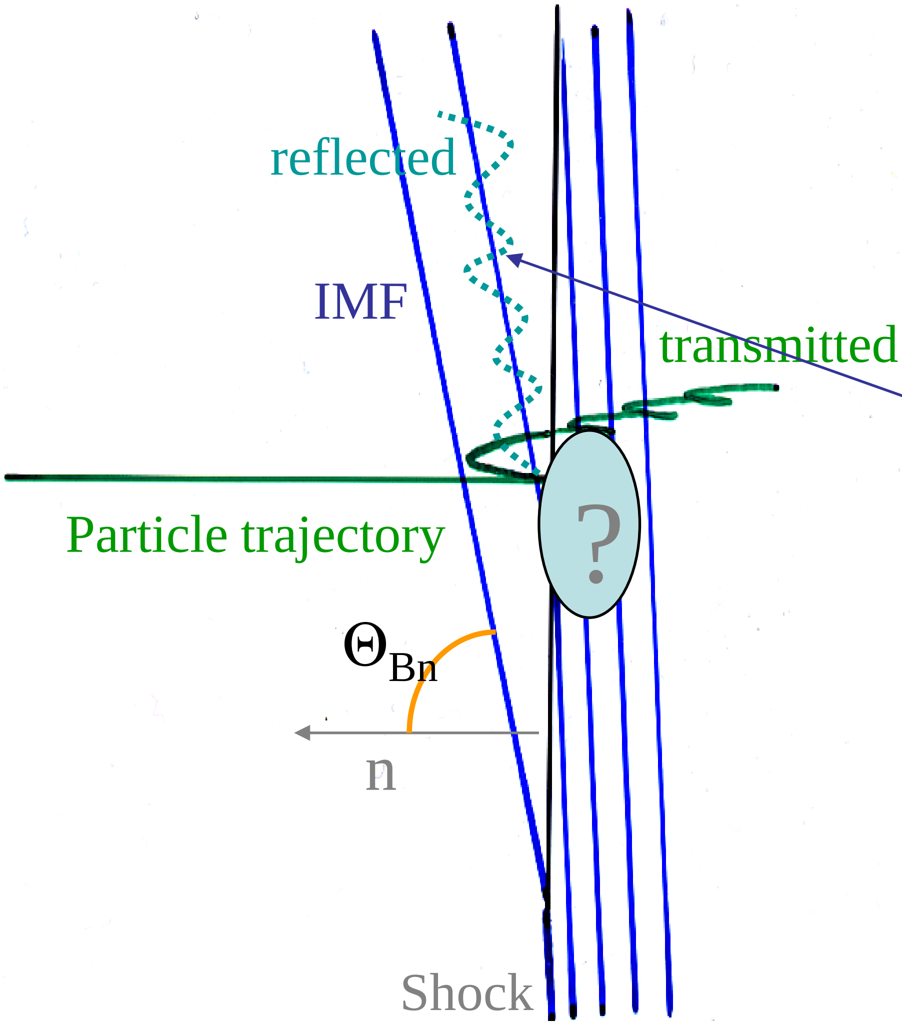

Field lines are convected downsteam

Particles can escape upstream if their velocity parallel to B exceeds convection speed

Kucharek et al. 2004

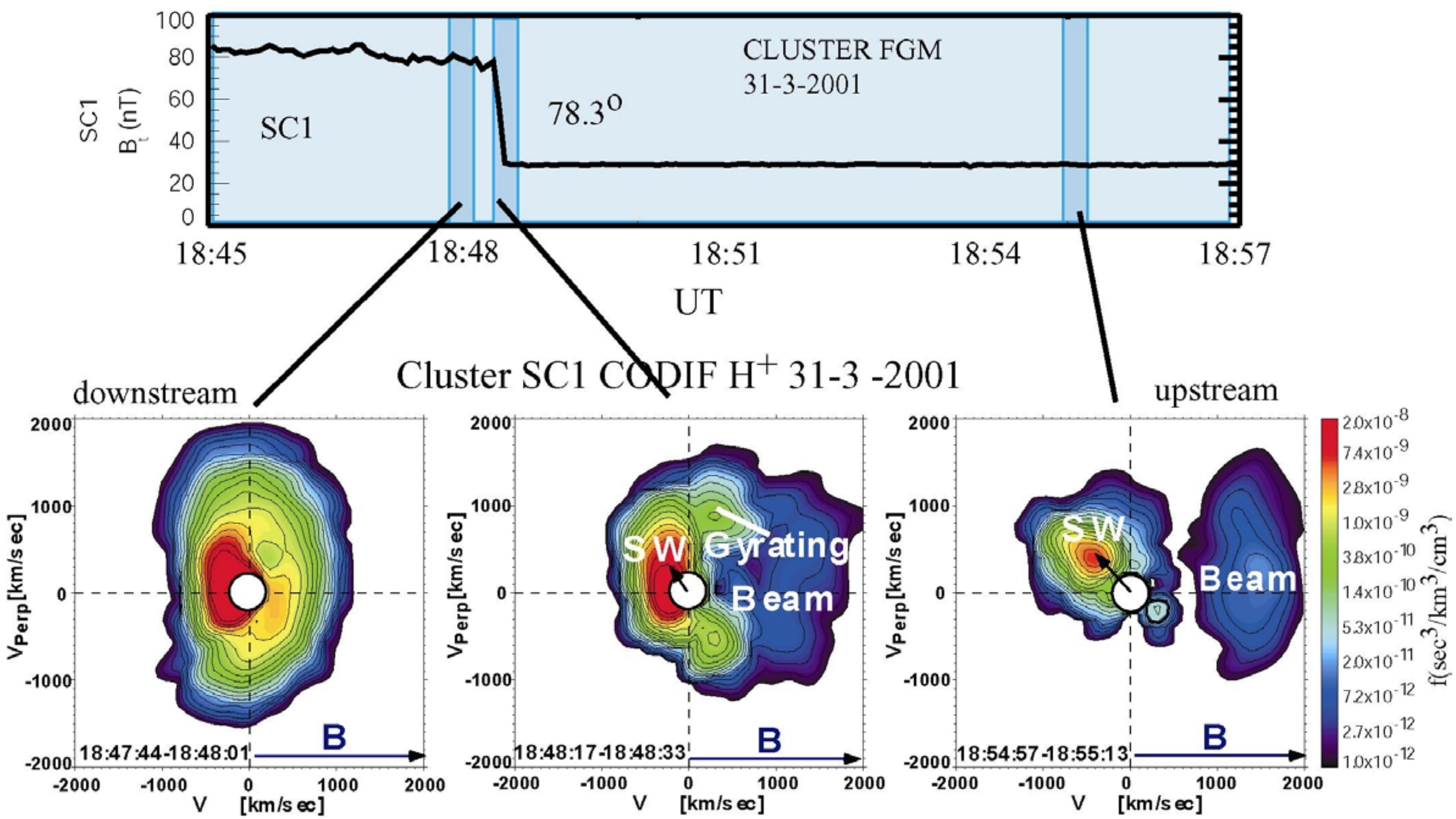

No or very small phase space density found downstream of the ramp at position of beam ions

Field-aligned beam seems to emerge from the ramp and NOT from downstream

Test particles in hybrid simulations of a quasi-perpendicular shock

Burgess 1987

Θ_{Bn}

40°

45°

50°

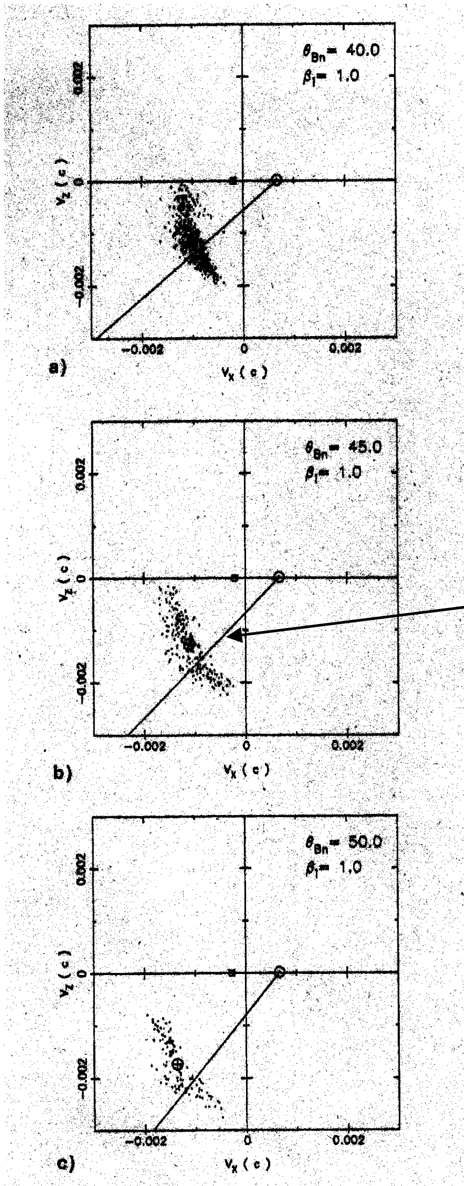

Simulation beams in v_x-v_z phase space as the angle Θ_{Bn} is increased. The line is the direction of the upstream magnetic field.

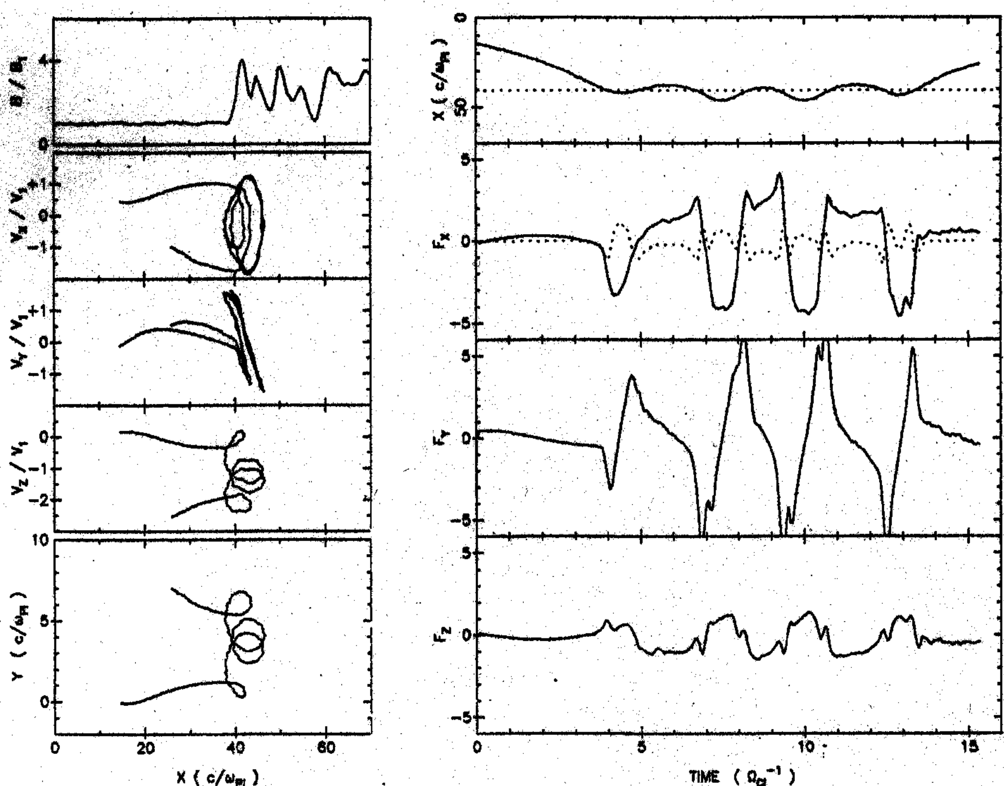

Trajectory of a directly reflected particle plotted in the shock frame. Top left: typical magnetic field trace. Right panels: time history of position and component forces.

Simulation beam density as a function of Θ_{Bn} for various values of upstream ion β (ratio of incident particle flux to backstreaming beam flux).

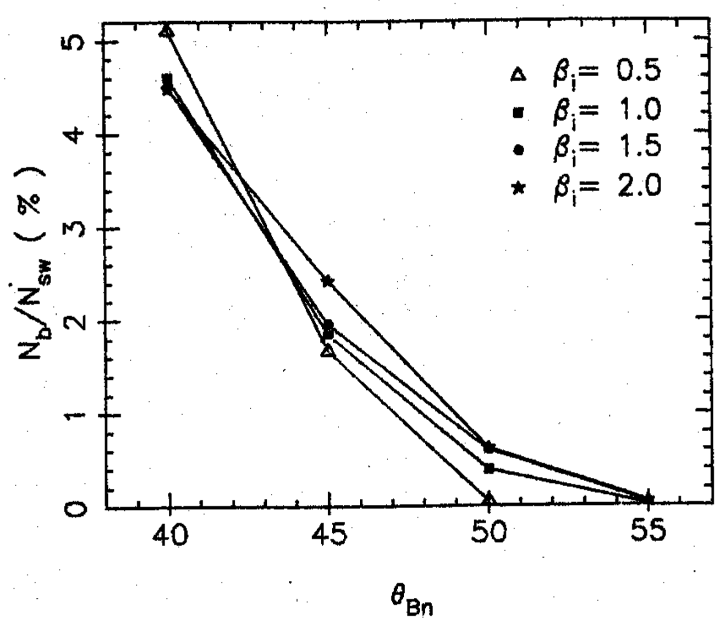

Summary

1. Quasi-Parallel Shocks

Upstream waves by r. h. resonant ion/ion beam instability

Waves at higher Mach number downstream directed group velocity

Mode conversion of upstream waves downstream

Interface instability – important at higher Mach number

Oblique shocks: waves develop into short large amplitude magnetic structures

Backstreaming ions: injection by energy gain at shock

2. Quasi-Perpendicular Shocks

Specularly reflected ions – Alfven ion cyclotron instability downstream

Ripples at shock surface parallel and perpendicular to magnetic field

Self-reformation (micro-instabilities in the foot, nonlinear whistler, whistler induced beam Instability)

Buneman instability in the foot of high Mach number shocks – electron acceleration

Field-Aligned Beams

Future Simulatios

1. Higher spatial dimensions:

   3-D in hybrid (takes into accound cross-field diffusion, shock rippling)
   2-D in PIC (allow for oblique k vectors of micro-instabilities in foot – many more istabilities – electron heating)

2. Realistic ion/electron mass ratio and large electron plasma/gyrofrequency in PIC simulations

3. Curved shocks (in particular study influence of quasi-perpendicular shock on quasi-parallel foreshock)

4. Minor ions, in particular pickup ions (heliospheric termination shock)